Verapamil-sensitive transport of quinacrine and methylene blue via mutant PfCRT reduces the malaria parasite's susceptibility to these tricyclic drugs

*Donelly A. van Schalkwyk[1,a,b], Megan N. Nash[1,a], Sarah H. Shafik[1,a], Robert L. Summers[1], Adele M. Lehane[1], Peter J. Smith[2], and Rowena E. Martin[1]**

[1]Research School of Biology, Australian National University, Canberra, ACT, 2601, Australia

[2]Division of Pharmacology, Department of Medicine, University of Cape Town, Private Bag, Rondebosch, 7701, South Africa

[a]D. A. vS., M. N. N., and S. H. S. contributed equally to this work.

[b]Present affiliation/address: Department of Immunology and Infection, Faculty of Infectious and Tropical Diseases, London School of Hygiene and Tropical Medicine, United Kingdom (D. A. vS.).

*Correspondence: Rowena Martin, Research School of Biology, Australian National University, Canberra, ACT, 2601, Australia (rowena.martin@anu.edu.au).

Running title: Transport of tricyclic drugs via PfCRT

Abstract: 200 words

Main text: 3493 words

Title: 150 characters and spaces

Running title: 38 characters and spaces

References: 50

Footnote Page

1)

Potential conflicts of interest: The authors do not have a commercial or other association that might pose a conflict of interest.

2)

Financial support: This work was supported by the Australian National Health and Medical Research Council (grant 1007035 and fellowship 1053082 to R.E.M. and fellowship 585519 to A.M.L.), the University of Cape Town Research Committee (D.A.vS. and P.J.S.), the Medical Research Council of South Africa (D.A.vS. and P.J.S.), and the L'Oréal Australia *For Women in Science* program (R.E.M.). S.H.S. and R.L.S. were supported by Australian Postgraduate Awards and R.L.S. also held an ANU PhD Supplementary Scholarship.

3)

This study, or part thereof, has not been presented at a meeting.

4)

*Correspondence: Rowena Martin, Research School of Biology, Australian National University, Canberra, ACT, 2601, Australia (rowena.martin@anu.edu.au). Telephone: +61 2 6197 0051; Fax: +61 2 6125 0313.

5)

[b]Present affiliation/address: Department of Immunology and Infection, Faculty of Infectious and Tropical Diseases, London School of Hygiene and Tropical Medicine, United Kingdom (D. A. vS.).

ABSTRACT

Background. It is becoming increasingly apparent that certain mutations in the *Plasmodium falciparum* 'chloroquine resistance transporter' (PfCRT) alter the parasite's susceptibility to diverse compounds. Here we investigated the interaction of PfCRT with three tricyclic compounds that have been used to treat malaria (quinacrine (QC) and methylene blue (MB)) or to study *P. falciparum* (acridine orange; AO).

Methods. We measured the antiplasmodial activities of QC, MB, and AO against chloroquine-resistant and chloroquine-sensitive *P. falciparum*, and determined whether QC and AO affect the accumulation and activity of chloroquine in these parasites. We also assessed the ability of mutant ($PfCRT^{Dd2}$) and wild-type ($PfCRT^{D10}$) variants of the protein to transport QC, MB, and AO when expressed at the surface of *Xenopus laevis* oocytes.

Results. Chloroquine-resistance conferring isoforms of PfCRT reduced the sensitivity of the parasite to QC, MB, and AO. In chloroquine-resistant (but not chloroquine-sensitive) parasites, AO and QC increased the parasite's accumulation of, and susceptibility to, chloroquine. All three compounds were shown to bind to $PfCRT^{Dd2}$, and the transport of QC and MB via this protein was saturable and inhibited by the chloroquine 'resistance-reverser' verapamil.

Conclusions. Our findings reveal that the $PfCRT^{Dd2}$-mediated transport of tricyclic antimalarials reduces the parasite's susceptibility to these drugs.

Keywords. Drug resistance; *Plasmodium falciparum;* tricyclic drug; methylene blue; PfCRT; fluorescent uptake assay; *Xenopus* oocytes.

INTRODUCTION

The global campaign to control and eliminate malaria is under serious threat from the emergence and spread of *Plasmodium falciparum* parasites that are resistant to the existing antimalarial drugs [1]. The *P. falciparum* chloroquine resistance transporter (PfCRT) plays a significant role in the phenomenon of drug resistance; mutations in this protein confer resistance to the former 'wonder drug' chloroquine (CQ) and also affect the parasite's susceptibility to a diverse range of molecules, including many of the drugs that have been – or are currently – deployed as antimalarials [e.g., [2] and reviewed in [3]].

PfCRT is located at the membrane of the parasite's digestive vacuole (DV) [4, 5]. Many quinoline-related drugs, including CQ and quinine, accumulate within this acidic compartment (pH 5-5.5) via 'weak-base trapping' [6]. Here they exert an antimalarial effect by preventing the conversion of toxic heme monomers, arising from the parasite's digestion of host hemoglobin, into the inert crystal hemozoin [7, 8]. Resistance to CQ and quinine is associated with a reduction in the accumulation of these drugs in the DV, and several biochemical studies produced indirect evidence for this being attributable to the efflux of CQ and quinine via mutant PfCRT [9-12]. A direct demonstration of this activity was achieved when the wild-type PfCRT ($PfCRT^{D10}$) and a resistance-conferring isoform of the protein ($PfCRT^{Dd2}$) were expressed in *Xenopus laevis* oocytes; $PfCRT^{Dd2}$ was shown to possess significant CQ and quinine transport activity, whereas $PfCRT^{D10}$ did not [13-15]. These findings aside, much remains to be understood about the protein's ability to recognize and transport diverse compounds.

Here we investigated interactions of PfCRT with quinacrine (QC), methylene blue (MB), and acridine orange (AO). All three molecules contain a tricyclic scaffold (Supplementary Figure 1) and will sequester within the DV due to weak-base trapping or, in the case of the

cationic MB, via weak-base trapping and/or oxidation of the reduced forms of the drug [16-19].

AO has been employed as a fluorescent dye for the diagnosis of malaria [20] and as a probe for estimating the pH of the DV (pH_{DV}) in CQ-sensitive and CQ-resistant parasites [21-23]. The latter studies reported that CQ-resistant strains have a lower pH_{DV} than their CQ-sensitive counterparts (pH 5.21 versus pH 5.64), and that this could account for the differential accumulation of, and susceptibility to, CQ between these parasites. Alternatively, it has been suggested that the observed difference in the accumulation of AO may instead be due to its export from the DV via mutant PfCRT [24].

MB was the first synthetic antimalarial drug and QC, which was derived from MB, was the first synthetic antimalarial to be widely used. Both drugs are thought to inhibit heme detoxification [17, 18, 25], with the redox-cycling capacity of MB potentially exerting an additional parasiticidal effect [18, 26]. Although QC was set aside following the introduction of CQ, structural derivatives of QC have since been deployed (pyronaridine) or are undergoing development [27, 28] as antimalarials. Interest in MB, which until recently was a largely overlooked antimalarial, has been greatly revived by studies that have found it to be (1) a potent gametocytocidal and transmission-blocking agent [29, 30], (2) a potential partner drug that improves the clinical efficacy of amodiaquine and artesunate-amodiaquine [31, 32], and (3) a relatively well-tolerated drug [31-33].

A number of in vitro studies have observed cross-resistance between QC and CQ [34-36] and these observations, along with the finding that QC increases the accumulation of CQ in CQ-resistant but not CQ-sensitive parasites [37], implicate mutations in PfCRT as a determinant of the parasite's susceptibility to QC. The relationship between CQ and MB susceptibility in CQ-resistant *P. falciparum* is considerably less clear. Several studies have reported that CQ resistance (and specifically mutant PfCRT) does not impart cross-resistance to MB [38-40], whereas others have observed modest but significant positive correlations

between the half-maximal inhibitory concentrations (IC_{50}s) of CQ and MB in *P. falciparum* [17, 41, 42].

We have sought to elucidate the mechanisms underpinning these observations by ascertaining the nature and strength of the interactions between PfCRT and QC, MB, and AO. Our findings reveal that CQ resistance-conferring isoforms of PfCRT reduce the parasite's susceptibility to tricyclic compounds and that, at least in the cases of QC and MB, this phenomenon is due to the ability of mutant PfCRT to transport these drugs away from their main site of action.

MATERIALS AND METHODS

Culture of *P. falciparum*-infected Erythrocytes

The use of human blood in this study was approved by the Australian National University's Human Research Ethics Committee. Two CQ-sensitive strains (D10 and 3D7), three CQ-resistant strains (K1, RSA11, and Dd2), and three *pfcrt* transfectant lines ($C2^{GC03}$, $C4^{Dd2}$, and $C6^{7G8}$; [43]) were cultured and synchronized as described previously [12].

P. falciparum Drug Susceptibility and Drug Accumulation

Measurements of parasite proliferation, and of [^{3}H]CQ and [^{3}H]AO in accumulation in trophozoite-infected erythrocytes, were performed according to the protocols provided in the Supplementary Materials.

Drug Transport in *Xenopus* Oocytes Expressing PfCRT

Oocytes were harvested and prepared using the method described in detail in the Supplementary Materials. $PfCRT^{Dd2}$ and $PfCRT^{D10}$ were expressed at the oocyte plasma membrane using an approach outlined elsewhere [13]. The uptake into oocytes of [^{3}H]CQ, as

well as that of unlabelled QC, MB, and AO (all of which fluoresce), was measured using the protocols described in the Supplementary Materials.

Statistics

Statistical comparisons were made using the Student's *t*-test for paired or unpaired samples, or ANOVA in conjunction with Tukey's multiple comparisons test.

RESULTS

Mutant Forms of PfCRT Decrease the Susceptibility of *P. falciparum* to QC, MB, and AO

The antiplasmodial activities of QC, MB and AO were evaluated in vitro against erythrocytes infected with field-derived CQ-sensitive (D10 or 3D7) or CQ-resistant (RSA11, K1, or Dd2) *P. falciparum* strains. The D10 and 3D7 strains carry the wild-type version of PfCRT ($PfCRT^{D10}$), K1 and Dd2 parasites carry resistance-conferring isoforms of the protein ($PfCRT^{K1}$ and $PfCRT^{Dd2}$, respectively), and the PfCRT haplotype carried by RSA11 is currently unknown. CQ was included as a reference drug and the resulting IC_{50}s are presented in Table 1. QC and MB displayed potent antiplasmodial activities, with IC_{50}s against 3D7 parasites of approximately 10 and 2.5 nM, respectively. However, these values increased 1.6 to 2-fold when the drugs were tested against the Dd2 strain. AO was the least active of the test compounds, with IC_{50}s of ~300 nM against the D10 and 3D7 strains, and these values also increased 1.9 to 2.3-fold in the CQ-resistant strains. The role of PfCRT in the observed decrease in the sensitivities of the CQ-resistant strains to QC, MB, and AO was investigated using a set of isogenic transfectant lines [43], which express the wild-type *pfcrt* allele ($C2^{GC03}$) or a mutant *pfcrt* allele from either Dd2 ($C4^{Dd2}$) or the CQ-resistant strain 7G8 ($C6^{7G8}$). Consistent with what was observed for the field-derived strains, the IC_{50}s determined for QC, MB, AO, and CQ were higher in the CQ-resistant lines ($C4^{Dd2}$ and $C6^{7G8}$) than in the CQ-sensitive $C2^{GC03}$ line (Table 1). CQ-resistant

parasites can be partially re-sensitised to CQ in vitro by verapamil (VP) or chlorpheniramine (CP) ([44] and Table 1) – a phenomenon we have shown to be attributable to the ability of these drugs to inhibit CQ transport via mutant PfCRT [13, 14, 45]. In the data presented in Table 1, the presence of 1 μM VP decreased the QC and MB IC_{50}s in all of the CQ-resistant strains and lines, and was without effect in their drug-sensitive counterparts. Taken together, these findings suggested that the decreased sensitivity of CQ-resistant parasites to QC and MB was due to the interaction of these drugs with mutant isoforms of PfCRT.

VP did not have a significant effect on the activity of AO in any of the parasite types (Table 1). We therefore explored the interaction between AO and PfCRT further by testing whether AO, like VP or CP, potentiates the activity of CQ against CQ-resistant parasites. An initial experiment revealed that the presence of 250 nM AO or 1 μM VP decreased the CQ IC_{50} in the K1 strain by ~30% and 65%, respectively, whereas no significant change was observed in the 3D7 strain (Supplementary Table 1). Isobolograms describing the interactions of CQ with AO, and of VP with AO, against the $C2^{GCO3}$ and $C4^{Dd2}$ lines indicated these combinations are additive in $C2^{GCO3}$ parasites, whereas interactions suggestive of synergism were observed in the $C4^{Dd2}$ line (Figure 1). These results suggested that the antiplasmodial activity of combinations of AO with CQ or VP is dependent on the *pfcrt* allele expressed and that AO may behave as a reverser of CQ resistance.

QC and AO Increase [^{3}H]CQ Accumulation in CQ-resistant Parasites

The resistance-reversing activity of VP causes an increase in the accumulation of [^{3}H]CQ in CQ-resistant strains, with no such change occurring in drug-sensitive parasites [44]. To investigate whether AO enhances the effects of CQ via the same mechanism, [^{3}H]CQ accumulation was measured in CQ-sensitive and CQ-resistant parasites in the presence or absence of AO, QC, and VP. We found that AO and QC increased the accumulation of [^{3}H]CQ in CQ-resistant parasites when present at 100 nM and 1 μM, respectively (Figure 2). By contrast,

1 μM AO had no effect on [^{3}H]CQ accumulation in the drug-sensitive parasites, whereas 100 nM QC caused a modest decrease in [^{3}H]CQ accumulation. The latter result suggests that QC reduces the amount of free heme, and therefore CQ-binding sites, within the DV of drug-sensitive parasites, whereas the observed increase in [^{3}H]CQ accumulation in the resistant line indicates that QC possesses a degree of resistance-reversing activity. Moreover, the finding that 1 μM AO and 5 μM VP increased the accumulation of [^{3}H]CQ in the C4^{Dd2} line to similar extents (Figure 2*D*) further supported the hypothesis that AO potentiates the activity of CQ against CQ-resistant parasites by blocking the PfCRT-mediated efflux of CQ from the DV.

QC, MB, and AO Inhibit the Transport of [^{3}H]CQ via PfCRT^{Dd2}

Direct measurements of the abilities of QC, MB, and AO to block CQ transport via PfCRT^{Dd2} were undertaken using the *Xenopus* oocyte system. In a preliminary assay in which the tricyclic compounds were each tested at 500 μM, QC and AO caused pronounced reductions in the PfCRT^{Dd2}-mediated transport of CQ, whereas MB caused a modest level of inhibition (Figure 3*A*). An analysis of the concentration-dependence of inhibition yielded IC_{50}s of 13.5 ± 0.9 μM, 41.0 ± 5.1 μM, and 1.3 ± 0.2 mM for QC, AO, and MB, respectively (Figures 3*B*-*D*).

QC and MB are Substrates of PfCRT^{Dd2}

We further investigated the nature of the interactions of PfCRT^{Dd2} with QC, MB, and AO by performing direct measurements of transport in the *Xenopus* oocyte system. We achieved this by re-purposing the radioisotope influx assay for the detection of fluorescent substrates (see Supplementary Materials). In all cases, there was a linear relationship between concentration and fluorescence intensity for QC, MB, and AO (Supplementary Figure 2). It was therefore possible to use the native fluorescence of these compounds to measure their uptake into oocytes expressing different forms of PfCRT.

Oocytes expressing PfCRT^{Dd2} were found to accumulate significantly more QC and MB than either non-injected oocytes or oocytes expressing PfCRT^{D10}, consistent with PfCRT^{Dd2}, but not PfCRT^{D10}, mediating the transport of these tricyclic drugs (Figures 4*A* and 5*A*; $P<0.001$ at 60 minutes). The uptake of QC and MB via PfCRT^{Dd2} was linear over time for at least 2 hours (Figures 4*B* and 5*B*) and the estimated rates of PfCRT^{Dd2}-mediated transport (in picomoles hour^{-1} per oocyte) were 7.01 ± 1.34 (QC) and 4.73 ± 0.14 (MB). An analysis of the concentration-dependence of QC and MB uptake revealed, in both cases, that the component of transport attributable to PfCRT^{Dd2} was saturable (Figures 4*C* and 5*C*). A least squares fit of the Michaelis-Menten equation to the data (Figures 4*D* and 5*D*) yielded apparent Michaelis constants (K_m) of 9.8 ± 1.1 and 123 ± 11.5 μM and maximal velocities (V_{max}) of 16.3 ± 0.7 and 202 ± 5 picomoles hour^{-1} per oocyte for QC and MB, respectively. By comparison, in non-injected oocytes and those expressing PfCRT^{D10}, the rate of QC and MB influx increased in a roughly linear manner with increasing concentrations of the drug (Figures 4*C* and 5*C*). This finding, together with the observation that these two oocyte types took up QC or MB to similarly low levels, indicates that this component of accumulation is due to the simple diffusion of the uncharged drug into the oocyte.

Several known inhibitors of PfCRT^{Dd2} were tested for their effect on QC and MB uptake in oocytes expressing PfCRT^{D10} or PfCRT^{Dd2}, including VP (250 μM), CQ (750 μM), neurotensin fragment 8-13 (NT; 250 μM) and, in the case of MB uptake, saquinavir (SQV; 250 μM) – which is the most potent of the inhibitors tested [46]. None of the test compounds affected the accumulation of QC or MB in the PfCRT^{D10}-expressing oocytes (Figures 4*E* and 5*E*). By contrast, VP reduced the PfCRT^{Dd2}-mediated uptake of QC and MB by 86 ± 1.6 and 65 ± 4 percent, respectively, and SQV caused a 71 ± 3 percent decrease in the transport of MB via PfCRT^{Dd2} (Figures 4*F* and 5*F*). Compared with VP, CQ and NT were less potent inhibitors of QC transport (71 ± 3 and 48 ± 4 percent decreases, respectively) and caused only modest reductions in the PfCRT^{Dd2}-mediated uptake of MB (30 ± 5 and 33 ± 2 percent decreases,

respectively).

Attempts to detect the transport of AO (75 or 150 μM) via PfCRT were performed at pH 4.5, 5.0, 5.5, and 6.0, and a second series of experiments also made measurements of [^{3}H]AO transport over the same pH range. Although several of the assays conducted at pH 5.0 appeared to detect a small increase in AO accumulation in the PfCRT^{Dd2}-expressing oocytes, the signal was not reproduced in the majority of the assays carried out. This suggested that AO is either not a substrate of PfCRT^{Dd2} or that the protein has a very low capacity for AO transport, such that – at least in the oocyte system – it is obscured by the rate of uptake via simple diffusion of the uncharged species (the proportion of AO in the uncharged form is relatively high, even at pH 5.0; Supplementary Table 2). The first scenario raised the possibility that PfCRT^{Dd2} (and PfCRT^{7G8}) decreases the parasite's susceptibility to AO without mediating the efflux of AO from the DV. We therefore compared the accumulation of [^{3}H]AO between the C2^{GC03}, C4^{Dd2}, and C6^{7G8} lines and found there to be a modest but significant decrease in [^{3}H]AO accumulation in the CQ-resistant lines (Figure 6). Consistent with the observed failure of VP to increase the activity of AO against CQ-resistant parasites, VP did not produce a PfCRT-dependent increase in the accumulation of [^{3}H]AO (data not shown) and assays performed with the CQ resistance-reverser CP suggest it may, if anything, cause a small decrease in [^{3}H]AO accumulation in the CQ-resistant lines (Supplementary Figure 3).

DISCUSSION

PfCRT is a significant player in the malaria parasite's steadily expanding resistance to antimalarial drugs, yet relatively little is understood about the extent of its substrate-specificity or the pharmacology of its transport activity. In this study, assays conducted with isogenic transfectant lines, which differ only in the isoform of PfCRT they express, revealed that CQ resistance-conferring isoforms of PfCRT confer a VP-sensitive decrease in the

parasite's susceptibility to the tricyclic drugs QC and MB. Characterization of the interaction of these drugs with a mutant isoform of PfCRT ($PfCRT^{Dd2}$) in the *Xenopus* oocyte system provided a mechanistic explanation for this phenomenon; $PfCRT^{Dd2}$ can efflux QC and MB out of the parasite's DV and VP inhibits this transport activity. Our findings are also consistent with QC and MB exerting their main schizontocidal activity within the DV, where they are thought to prevent the detoxification of heme and where MB is also likely to disrupt vital redox processes.

We also found that parasites carrying a mutant isoform of PfCRT accumulated less of the pH probe AO, and were more resistant to its antiplasmodial activity, than parasites carrying the wild-type version of PfCRT – but these phenomena were not affected by VP. AO did, however, behave as a CQ resistance-reverser; it inhibited CQ transport via $PfCRT^{Dd2}$ in the oocyte system (IC_{50} of 41 μM) and chemosensitized CQ-resistant parasites to CQ. The simplest explanation for these observations is that AO binds to mutant PfCRT and is translocated at a low rate, such that it is not consistently detected above the simple diffusion of uncharged AO into the oocyte. These findings render AO unsuitable for comparing the pH_{DV} between CQ-sensitive and CQ-resistant parasites, since the efflux of the probe via mutant PfCRT will result in non-pH-dependent changes in the accumulation of AO. Indeed, no significant difference was observed between CQ-sensitive and CQ-resistant parasites when the pH_{DV} was measured with several other pH-sensitive dyes [24].

Our characterization of the interactions between mutant PfCRT and QC in the oocyte system revealed QC transport via $PfCRT^{Dd2}$ to be a high-affinity and low-capacity process (e.g., K_m(QC) of 9.8 μM compared with K_m(CQ) of 232-245 μM [13, 15]) and QC to be a strong inhibitor of the $PfCRT^{Dd2}$-mediated transport of CQ (QC is comparable in potency to SQV; IC_{50}s of 13.5 and 13 μM [46], respectively). These data, which indicate that QC can outcompete CQ for transport via $PfCRT^{Dd2}$, provide a mechanistic explanation for the ability of QC to increase [^{3}H]CQ accumulation in CQ-resistant parasites.

The finding that the parasite's sensitivity to MB is reduced by the PfCRT-mediated resistance mechanism is consistent with several studies in which a significant correlation between MB and CQ susceptibilities was observed in *P. falciparum* [17, 41, 42], but is at odds with reports of there being no such relationship [38-40]. The basis for this difference is not clear, but may relate to differences in the parasite proliferation protocols between labs. For example, even when the same parasite strains were studied (CQ-sensitive 'D6' and CQ-resistant 'W2'), one group observed modest but significant cross-resistance between CQ and MB [17] whereas another did not [39]. We found $PfCRT^{Dd2}$ to be a medium-affinity and very high-capacity transporter of MB (e.g., the V_{max} values (in picomoles $hour^{-1}$ per oocyte) for MB and CQ are 202 and 61-67 [13, 15], respectively), which may explain, at least in part, why VP and CP inhibited MB uptake to a much lesser extent than what was observed for QC uptake. However, it is also worth noting that MB was a very poor inhibitor of CQ uptake (IC_{50} of 1.3 mM) and vice versa. We recently provided evidence for there being at least two distinct, but antagonistically-interacting, substrate-binding sites within $PfCRT^{Dd2}$ and proposed this region of the transporter most likely resembles a cavity with multiple points for substrate interaction [14]. Hence, the relatively poor ability of MB and CQ to interfere with each other's transport could arise from these two drugs binding to largely different sets of attachment points. Likewise, the inability of VP to decrease the AO IC_{50} (and of CP to increase [^{3}H]AO accumulation) in CQ-resistant parasites may be due to there being little or no overlap between the attachment points occupied by AO and VP (or CP).

The high-capacity transport of MB via mutant PfCRT, and the resulting reduction in the parasite's susceptibility to the drug, could have future clinical relevance given the potential of MB to serve as a potent transmission-blocking agent and its inclusion in two candidate combination therapies (artesunate-amodiaquine-MB and amodiaquine-MB). It is conceivable that parasites carrying mutant isoforms of PfCRT will be selected by MB-containing treatments, forming a population from which high-level resistance could evolve. Whether this

transpires will depend on a number of parameters (none of which are currently known), such as the approximate concentration of MB within the DV and the extent to which it can be lowered by mutant PfCRT, how this fluctuates during the treatment course, and for what period the level of MB within the DV falls beneath the minimum parasiticidal concentration. Moreover, these factors are likely to be affected by the co-administration of MB with amodiaquine, since the latter is suspected to be a substrate of mutant PfCRT [12, 47]. It is also possible that the gametocytocidal activity of MB could be affected by the PfCRT-mediated resistance mechanism; although mature gametocytes no longer digest hemoglobin, they retain both PfCRT as well as vesicles that could be the remnant of, or replacement for, the DV [48, 49].

The data presented here have (1) broadened the known substrate range of mutant PfCRT to include tricyclic compounds and (2) established that the PfCRT-mediated efflux of QC and MB from the DV decreases the parasite's sensitivity to these molecules. When taken together with previous studies [13-15], these results reveal a shared mechanism of resistance for CQ, quinine, quinidine, QC, and MB. Our work therefore adds further support to the proposal that PfCRT behaves as a 'multidrug resistance carrier' [3, 50] and highlights the potential for there being an interaction between mutant PfCRT and existing and upcoming antimalarials with quinoline- and acridine-related structures (e.g., ferroquine and pyronaridine).

FIGURE LEGENDS

Figure 1. Isobolograms describing the interactions of verapamil (VP) with chloroquine (CQ), acridine orange (AO) with CQ, and VP with AO, against erythrocytes infected with $C2^{GCO3}$ or $C4^{Dd2}$ parasites. The data represent the mean ± SEM from 3 independent experiments (performed on different days), within which measurements were averaged from 3 replicates. Where not shown, error bars fall within the symbols. In general, a fractional inhibitory concentration (FIC) of 1.0 suggests that the effects of the two compounds are additive, a FIC ≤ 0.5 suggests synergism, and a FIC ≥ 4.0 indicates antagonism. The mean FICs for the $C2^{GCO3}$ line were as follows: VP and CQ combination, 1.04; AO and CQ combination, 1.00; VP and AO combination, 0.99. None of these FICs appeared different from 1.0, consistent with all three drug combinations being additive in the CQ-sensitive parasite line. The mean FICs for the $C4^{Dd2}$ line were as follows: VP and CQ combination, 0.54; AO and CQ combination, 0.94; VP and AO combination, 0.84. In all three cases, the mean FICs were below 1.0, but were also above the accepted threshold for categorizing an interaction as synergistic. This finding suggests that the drug combinations were slightly synergistic in the CQ-resistant parasite line.

Figure 2. Effects of quinacrine (QC), acridine orange (AO), and verapamil (VP) on the accumulation of radiolabelled chloroquine ([^{3}H]CQ) by erythrocytes infected with mature trophozoite-stage parasites. Panels *A*, *B*, and *C* show data for CQ-sensitive parasites ($C2^{GCO3}$, D10, and 3D7, respectively). Panels *D*, *E*, and *F* show data for CQ-resistant parasites ($C4^{Dd2}$, RSA11, and K1, respectively). CQ accumulation is expressed in terms of the fold difference in the [^{3}H]CQ 'distribution ratio', which corresponds to the concentration of [^{3}H]CQ within the infected cells relative to the concentration in the extracellular medium. In panels *A* and *D*, the data represent the mean + SEM from 6 independent experiments (performed on different days), within which measurements were averaged from 3 replicates. Panels *B*, *C*, *E*, and *F*

show the mean + range/2 of 2 independent experiments (performed on different days), within which measurements were averaged from 3 replicates. In panel *E*, the SEM for the 100 nM AO treatment was very small and the error bar is therefore not visible. The asterisks denote a significant difference in [^{3}H]CQ accumulation between the control treatment and that measured in the presence of QC, AO, or VP: *, $P < 0.05$; **, $P < 0.01$; ***, $P < 0.001$ (ANOVA).

Figure 3. Quinacrine (QC), acridine orange (AO), and methylene blue (MB) inhibit the transport of radiolabelled chloroquine ([^{3}H]CQ) via the *Plasmodium falciparum* chloroquine resistance transporter (PfCRT) in *Xenopus laevis* oocytes. *A*, [^{3}H]CQ uptake into oocytes expressing the Dd2 isoform of PfCRT ($PfCRT^{Dd2}$; black bars) or the D10 isoform of PfCRT ($PfCRT^{D10}$; white bars) in the presence of 500 μM unlabelled CQ, QC, AO, or MB. *B -D*, Concentration-dependent inhibition of the uptake of [^{3}H]CQ into oocytes expressing $PfCRT^{Dd2}$ (black circles) or $PfCRT^{D10}$ (white circles) by QC, AO, or MB. In all panels, [^{3}H]CQ uptake is expressed relative to that measured in the $PfCRT^{Dd2}$-expressing oocytes under control conditions. The data represent the mean ± SEM from 3 to 5 independent experiments (performed on different days and using oocytes from different frogs), within which measurements were made from 10 oocytes per treatment. Where not shown, error bars fall within the symbols. Note that non-injected oocytes and oocytes expressing $PfCRT^{D10}$ take up [^{3}H]CQ to similar (low) levels via simple diffusion of the neutral species; this represents the "background" level of CQ accumulation in oocytes. In panel *A*, the asterisks denote a significant difference in [^{3}H]CQ uptake between the control $PfCRT^{Dd2}$ treatment and that measured in the presence of CQ, QC, AO, or MB: ***, $P < 0.001$ (ANOVA). Abbreviation: IC_{50}, half-maximal inhibitory concentration.

Figure 4. Quinacrine (QC) transport properties of the *Plasmodium falciparum* chloroquine

resistance transporter (PfCRT) in *Xenopus laevis* oocytes. *A*, Oocytes expressing the Dd2 isoform of PfCRT ($PfCRT^{Dd2}$; black circles) showed a marked increase in QC accumulation relative to non-injected oocytes (black triangles) and to those expressing the D10 isoform of PfCRT ($PfCRT^{D10}$; white circles). Rates of QC uptake (picomoles $hour^{-1}$ per oocyte; $n = 3 \pm$ SEM, estimated from uptake at 60 minutes) were as follows: non-injected, 1.74 ± 0.37; $PfCRT^{D10}$, 1.50 ± 0.20; $PfCRT^{Dd2}$, 8.62 ± 1.58. *B*, The $PfCRT^{Dd2}$-mediated uptake of QC (obtained by subtracting the average of the uptake measured in non-injected and $PfCRT^{D10}$-expressing oocytes from that measured in $PfCRT^{Dd2}$-expressing oocytes) was approximately linear with time for at least 2 hours. The rate of QC transport via $PfCRT^{Dd2}$, estimated from uptake at 60 minutes, was 7.01 ± 1.34 picomoles $hour^{-1}$ per oocyte ($n = 3 \pm$ SEM). *C*, The effect of QC concentration on QC uptake by non-injected oocytes (black triangles) and oocytes expressing $PfCRT^{D10}$ (white circles) or $PfCRT^{Dd2}$ (black circles). The accumulation of QC by the control oocytes increased linearly with increasing concentrations of QC, although a second component – attributable perhaps to the binding of QC to the oocyte surface – may have been present below 2.5 μM. *D*, The concentration-dependence of the $PfCRT^{Dd2}$-mediated transport of QC (in picomoles $hour^{-1}$ per oocyte). *E*, Uptake of QC into oocytes expressing $PfCRT^{D10}$ (white bars) or $PfCRT^{Dd2}$ (black bars) in the presence of 750 μM chloroquine (CQ), 250 μM verapamil (VP), or 250 μM neurotensin (NT). *F*, Inhibition of the $PfCRT^{Dd2}$-mediated transport of QC by VP, CQ, or NT. The extracellular concentration of QC was 40 μM (panels A and B), 2.5-40 μM (panels C and D), or 10 μM (panels E and F). In all panels except *D*, QC uptake is expressed relative to that measured in the relevant $PfCRT^{Dd2}$ control. The data represent the mean ± SEM from 3 to 11 independent experiments (performed on different days and using oocytes from different frogs), within which measurements were made from 12 oocytes per treatment. Where not shown, error bars fall within the symbols. In panels *E* and *F*, the asterisks denote a significant difference in QC uptake between the control $PfCRT^{Dd2}$ treatment and that measured in the presence of VP, CQ, or NT: ***, $P < 0.001$ (ANOVA).

Abbreviations: K_m, apparent Michaelis constant; V_{max}, maximum velocity.

Figure 5. Methylene blue (MB) transport properties of the *Plasmodium falciparum* chloroquine resistance transporter (PfCRT) in *Xenopus laevis* oocytes. *A*, Oocytes expressing the Dd2 isoform of PfCRT ($PfCRT^{Dd2}$; black circles) showed a marked increase in MB accumulation relative to non-injected oocytes (black triangles) and to those expressing the D10 isoform of PfCRT ($PfCRT^{D10}$; white circles). Rates of MB uptake (picomoles $hour^{-1}$ per oocyte; $n = 3 \pm$ SEM, estimated from uptake at 60 minutes) were as follows: non-injected, 1.61 ± 0.07; $PfCRT^{D10}$, 1.59 ± 0.08; $PfCRT^{Dd2}$, 6.33 ± 0.22. *B*, The $PfCRT^{Dd2}$-mediated uptake of MB (obtained by subtracting the average of the uptake measured in non-injected and $PfCRT^{D10}$-expressing oocytes from that measured in $PfCRT^{Dd2}$-expressing oocytes) was approximately linear with time for at least 2 hours. The rate of MB transport via $PfCRT^{Dd2}$, estimated from uptake at 60 minutes, was 4.73 ± 0.14 picomoles $hour^{-1}$ per oocyte ($n = 3 \pm$ SEM). *C*, The effect of MB concentration on MB uptake by non-injected oocytes (black triangles) and oocytes expressing $PfCRT^{D10}$ (white circles) or $PfCRT^{Dd2}$ (black circles). The accumulation of MB by the control oocytes increased linearly with increasing concentrations of MB between 150 μM and 2 mM MB. A second component was observed below 150 μM; this probably reflects the binding of MB to the oocyte surface. *D*, The concentration-dependence of the $PfCRT^{Dd2}$-mediated transport of MB (in picomoles $hour^{-1}$ per oocyte). *E*, Uptake of MB into oocytes expressing $PfCRT^{D10}$ (white bars) or $PfCRT^{Dd2}$ (black bars) in the presence of 250 μM saquinavir (SQV), 750 μM chloroquine (CQ), 250 μM verapamil (VP), or 250 μM neurotensin (NT). *F*, Inhibition of the $PfCRT^{Dd2}$-mediated transport of MB by SQV, VP, CQ, or NT. The extracellular concentration of MB was 75 μM (panels A, B, E and F) or 0.025-2 mM (panels C and D). In all panels except *D*, MB uptake is expressed relative to that measured in the relevant $PfCRT^{Dd2}$ control. The data represent the mean ± SEM from 3 to 5 independent experiments (performed on different days and using oocytes from different frogs), within

404 which measurements were made from 12 oocytes per treatment. Where not shown, error
405 bars fall within the symbols. In panels *E* and *F*, the asterisks denote a significant difference in
406 MB uptake between the control $PfCRT^{Dd2}$ treatment and that measured in the presence of
407 SQV, VP, CQ, or NT: **, $P < 0.01$; ***, $P < 0.001$ (ANOVA). Abbreviations: K_m, apparent
408 Michaelis constant; V_{max}, maximum velocity.
409
410 **Figure 6.** Accumulation of radiolabelled chloroquine ([^{3}H]CQ) or radiolabelled acridine
411 orange ([^{3}H]AO) by erythrocytes infected with mature trophozoite-stage parasites. The white,
412 black, and gray bars show data for the $C2^{GCO3}$, $C4^{Dd2}$, and $C6^{7G8}$ parasite lines, respectively. The
413 accumulation of [^{3}H]drug was expressed as a 'distribution ratio' (i.e., the concentration of
414 [^{3}H]drug within the infected cells relative to the concentration in the extracellular medium)
415 and is shown relative to the ratio measured in the $C2^{GCO3}$ parasites. Under control conditions,
416 the distribution ratios for CQ and AO in the $C2^{GCO3}$ line were 773 ± 95 and 299 ± 31,
417 respectively. The data represent the mean + SEM of 4 independent experiments (performed
418 on different days), within which measurements were averaged from 2 replicates. The
419 asterisks denote a significant difference in [^{3}H]drug accumulation between the $C2^{GCO3}$ line and
420 that measured in the $C4^{Dd2}$ or $C6^{7G8}$ lines: *, $P < 0.05$; **, $P < 0.01$; ***, $P < 0.001$ (ANOVA, with
421 "experiment" nominated as a "blocking factor").
422
423 **Acknowledgements**
424 We thank Eileen Baker, Rachel Slatyer, and Tessa Attenborough for technical assistance, Prof
425 David Fidock for providing the transfectant *P. falciparum* lines, and the Canberra Branch of
426 the Australian Red Cross Blood Service for the provision of blood.
427
428 **References**
429

1. Ashley, E.A., M. Dhorda, R.M. Fairhurst, et al. Spread of artemisinin resistance in *Plasmodium falciparum* malaria. N Engl J Med **2014**; 371:411-23.
2. Yuan, J., K.C. Cheng, R.L. Johnson, et al. Chemical genomic profiling for antimalarial therapies, response signatures, and molecular targets. Science **2011**; 333:724-9.
3. Summers, R.L., M.N. Nash, R.E. Martin. Know your enemy: understanding the role of PfCRT in drug resistance could lead to new antimalarial tactics. Cell Mol Life Sci **2012**; 69:1967-95.
4. Fidock, D.A., T. Nomura, A.K. Talley, et al. Mutations in the *P. falciparum* digestive vacuole transmembrane protein PfCRT and evidence for their role in chloroquine resistance. Mol Cell **2000**; 6:861-71.
5. Cooper, R.A., M.T. Ferdig, X.Z. Su, et al. Alternative mutations at position 76 of the vacuolar transmembrane protein PfCRT are associated with chloroquine resistance and unique stereospecific quinine and quinidine responses in *Plasmodium falciparum*. Mol Pharmacol **2002**; 61:35-42.
6. Bray, P.G., M. Mungthin, I.M. Hastings, et al. PfCRT and the trans-vacuolar proton electrochemical gradient: regulating the access of chloroquine to ferriprotoporphyrin IX. Mol Microbiol **2006**; 62:238-51.
7. Mungthin, M., P.G. Bray, R.G. Ridley, S.A. Ward. Central role of hemoglobin degradation in mechanisms of action of 4-aminoquinolines, quinoline methanols, and phenanthrene methanols. Antimicrob Agents Chemother **1998**; 42:2973-7.
8. Fitch, C.D. Ferriprotoporphyrin IX, phospholipids, and the antimalarial actions of quinoline drugs. Life Sci **2004**; 74:1957-72.
9. Naude, B., J.A. Brzostowski, A.R. Kimmel, T.E. Wellems. *Dictyostelium discoideum* expresses a malaria chloroquine resistance mechanism upon transfection with mutant, but not wild-type, *Plasmodium falciparum* transporter PfCRT. J Biol Chem **2005**; 280:25596-25603.

10. Sanchez, C.P., J.E. McLean, P. Rohrbach, D.A. Fidock, W.D. Stein, M. Lanzer. Evidence for a *pfcrt*-associated chloroquine efflux system in the human malarial parasite *Plasmodium falciparum*. Biochemistry **2005**; 44:9862-70.

11. Lehane, A.M., K. Kirk. Chloroquine resistance-conferring mutations in *pfcrt* give rise to a chloroquine-associated H^+ leak from the malaria parasite's digestive vacuole. Antimicrob Agents Chemother **2008**; 52:4374-80.

12. Lehane, A.M., K. Kirk. Efflux of a range of antimalarial drugs and 'chloroquine resistance reversers' from the digestive vacuole in malaria parasites with mutant PfCRT. Mol Microbiol **2010; 77:1039-51**.

13. Martin, R.E., R.V. Marchetti, A.I. Cowan, S.M. Howitt, S. Bröer, K. Kirk. Chloroquine transport via the malaria parasite's chloroquine resistance transporter. Science **2009**; 325:1680-2.

14. Bellanca, S., R.L. Summers, M. Meyrath, et al. Multiple drugs compete for transport via the *Plasmodium falciparum* chloroquine resistance transporter at distinct but interdependent sites. J Biol Chem **2014**; 289:36336-51.

15. Summers, R.L., A. Dave, T.J. Dolstra, et al. Diverse mutational pathways converge on saturable chloroquine transport via the malaria parasite's chloroquine resistance transporter. Proc Natl Acad Sci U S A **2014**; 111:E1759-67.

16. Buchholz, K., R.H. Schirmer, J.K. Eubel, et al. Interactions of methylene blue with human disulfide reductases and their orthologues from *Plasmodium falciparum*. Antimicrob Agents Chemother **2008**; 52:183-91.

17. Atamna, H., M. Krugliak, G. Shalmiev, E. Deharo, G. Pescarmona, H. Ginsburg. Mode of antimalarial effect of methylene blue and some of its analogues on *Plasmodium falciparum* in culture and their inhibition of *P. vinckei petteri* and *P. yoelii nigeriensis in vivo*. Biochem Pharmacol **1996**; 51:693-700.

18. Blank, O., E. Davioud-Charvet, M. Elhabiri. Interactions of the antimalarial drug methylene blue with methemoglobin and heme targets in *Plasmodium falciparum*: a physico-biochemical study. Antioxid Redox Signal **2012**; 17:544-54.

19. Ginsburg, H., E. Nissani, M. Krugliak. Alkalinization of the food vacuole of malaria parasites by quinoline drugs and alkylamines is not correlated with their antimalarial activity. Biochem Pharmacol **1989**; 38:2645-54.

20. Keiser, J., J. Utzinger, Z. Premji, Y. Yamagata, B.H. Singer. Acridine Orange for malaria diagnosis: its diagnostic performance, its promotion and implementation in Tanzania, and the implications for malaria control. Ann Trop Med Parasitol **2002**; 96:643-54.

21. Bennett, T.N., A.D. Kosar, L.M. Ursos, et al. Drug resistance-associated pfCRT mutations confer decreased *Plasmodium falciparum* digestive vacuolar pH. Mol Biochem Parasitol **2004**; 133:99-114.

22. Ursos, L.M., S.M. Dzekunov, P.D. Roepe. The effects of chloroquine and verapamil on digestive vacuolar pH of *P. falciparum* either sensitive or resistant to chloroquine. Mol Biochem Parasitol **2000**; 110:125-34.

23. Dzekunov, S.M., L.M. Ursos, P.D. Roepe. Digestive vacuolar pH of intact intraerythrocytic *P. falciparum* either sensitive or resistant to chloroquine. Mol Biochem Parasitol **2000**; 110:107-24.

24. Hayward, R., K.J. Saliba, K. Kirk. The pH of the digestive vacuole of *Plasmodium falciparum* is not associated with chloroquine resistance. J Cell Sci **2006**; 119:1016-25.

25. Kumar, S., M. Guha, V. Choubey, P. Maity, U. Bandyopadhyay. Antimalarial drugs inhibiting hemozoin (beta-hematin) formation: a mechanistic update. Life Sci **2007**; 80:813-28.

26. Ehrhardt, K., E. Davioud-Charvet, H. Ke, A.B. Vaidya, M. Lanzer, M. Deponte. The antimalarial activities of methylene blue and the 1,4-naphthoquinone 3-[4-

(trifluoromethyl)benzyl]-menadione are not due to inhibition of the mitochondrial electron transport chain. Antimicrob Agents Chemother **2013**; 57:2114-20.

27. Kelly, J.X., M.J. Smilkstein, R. Brun, et al. Discovery of dual function acridones as a new antimalarial chemotype. Nature **2009**; 459:270-3.

28. Valdes, A.F. Acridine and acridinones: old and new structures with antimalarial activity. Open Med Chem J **2011**; 5:11-20.

29. Adjalley, S.H., G.L. Johnston, T. Li, et al. Quantitative assessment of *Plasmodium falciparum* sexual development reveals potent transmission-blocking activity by methylene blue. Proc Natl Acad Sci U S A **2011**; 108:E1214-23.

30. Coulibaly, B., A. Zoungrana, F.P. Mockenhaupt, et al. Strong gametocytocidal effect of methylene blue-based combination therapy against *falciparum* malaria: a randomised controlled trial. PLoS One **2009**; 4:e5318.

31. Zoungrana, A., B. Coulibaly, A. Sie, et al. Safety and efficacy of methylene blue combined with artesunate or amodiaquine for uncomplicated *falciparum* malaria: a randomized controlled trial from Burkina Faso. PLoS One **2008**; 3:e1630.

32. Coulibaly, B., M. Pritsch, M. Bountogo, et al. Efficacy and safety of triple combination therapy with artesunate-amodiaquine-methylene blue for *falciparum* malaria in children: a randomized controlled trial in Burkina Faso. J Infect Dis **2015**; 211:689-97.

33. Muller, O., F.P. Mockenhaupt, B. Marks, et al. Haemolysis risk in methylene blue treatment of G6PD-sufficient and G6PD-deficient West-African children with uncomplicated *falciparum* malaria: a synopsis of four RCTs. Pharmacoepidemiol Drug Saf **2013**; 22:376-85.

34. Anderson, M.O., J. Sherrill, P.B. Madrid, et al. Parallel synthesis of 9-aminoacridines and their evaluation against chloroquine-resistant *Plasmodium falciparum*. Bioorg Med Chem **2006**; 14:334-43.

35. Elueze, E.I., S.L. Croft, D.C. Warhurst. Activity of pyronaridine and mepacrine against twelve strains of *Plasmodium falciparum in vitro*. J Antimicrob Chemother **1996**; 37:511-8.

36. Hawley, S.R., P.G. Bray, M. Mungthin, J.D. Atkinson, P.M. O'Neill, S.A. Ward. Relationship between antimalarial drug activity, accumulation, and inhibition of heme polymerization in *Plasmodium falciparum in vitro*. Antimicrob Agents Chemother **1998**; 42:682-6.

37. Sanchez, C.P., J.E. McLean, W. Stein, M. Lanzer. Evidence for a substrate specific and inhibitable drug efflux system in chloroquine resistant *Plasmodium falciparum* strains. Biochemistry **2004**; 43:16365-73.

38. Pascual, A., M. Henry, S. Briolant, et al. *In vitro* activity of Proveblue (methylene blue) on *Plasmodium falciparum* strains resistant to standard antimalarial drugs. Antimicrob Agents Chemother **2011**; 55:2472-4.

39. Vennerstrom, J.L., M.T. Makler, C.K. Angerhofer, J.A. Williams. Antimalarial dyes revisited: xanthenes, azines, oxazines, and thiazines. Antimicrob Agents Chemother **1995**; 39:2671-7.

40. Okombo, J., S.M. Kiara, L. Mwai, et al. Baseline *in vitro* activities of the antimalarials pyronaridine and methylene blue against *Plasmodium falciparum* isolates from Kenya. Antimicrob Agents Chemother **2012**; 56:1105-7.

41. Wirjanata, G., B.F. Sebayang, F. Chalfein, et al. Potent *ex vivo* activity of naphthoquine and methylene blue against drug resistant clinical isolates of *Plasmodium falciparum* and *Plasmodium vivax*. Antimicrob Agents Chemother **2015**; 59:6117-24.

42. Akoachere, M., K. Buchholz, E. Fischer, et al. *In vitro* assessment of methylene blue on chloroquine-sensitive and -resistant *Plasmodium falciparum* strains reveals synergistic action with artemisinins. Antimicrob Agents Chemother **2005**; 49:4592-7.

556 43. Sidhu, A.B., D. Verdier-Pinard, D.A. Fidock. Chloroquine resistance in *Plasmodium*
557 *falciparum* malaria parasites conferred by *pfcrt* mutations. Science **2002**; 298:210-3.
558 44. Martin, S.K., A.M. Oduola, W.K. Milhous. Reversal of chloroquine resistance in
559 *Plasmodium falciparum* by verapamil. Science **1987**; 235:899-901.
560 45. Deane, K.J., R.L. Summers, A.M. Lehane, R.E. Martin, R.A. Barrow. Chlorpheniramine
561 Analogues Reverse Chloroquine Resistance in *Plasmodium falciparum* by Inhibiting
562 PfCRT. ACS Med Chem Lett **2014**; 5:576-81.
563 46. Martin, R.E., A.S. Butterworth, D.L. Gardiner, K. Kirk, J.S. McCarthy, T.S. Skinner-Adams.
564 Saquinavir inhibits the malaria parasite's chloroquine resistance transporter.
565 Antimicrob Agents Chemother **2012**; 56:2283-9.
566 47. Sa, J.M., O. Twu, K. Hayton, et al. Geographic patterns of *Plasmodium falciparum* drug
567 resistance distinguished by differential responses to amodiaquine and chloroquine.
568 Proc Natl Acad Sci U S A **2009**; 106:18883-9.
569 48. Hanssen, E., C. Knoechel, M. Dearnley, et al. Soft X-ray microscopy analysis of cell
570 volume and hemoglobin content in erythrocytes infected with asexual and sexual
571 stages of *Plasmodium falciparum*. J Struct Biol **2012**; 177:224-32.
572 49. Silvestrini, F., E. Lasonder, A. Olivieri, et al. Protein export marks the early phase of
573 gametocytogenesis of the human malaria parasite *Plasmodium falciparum*. Mol Cell
574 Proteomics **2010**; 9:1437-48.
575 50. Summers, R.L., R.E. Martin. Functional characteristics of the malaria parasite's
576 "chloroquine resistance transporter": implications for chemotherapy. Virulence **2010**;
577 1:304-8.
578

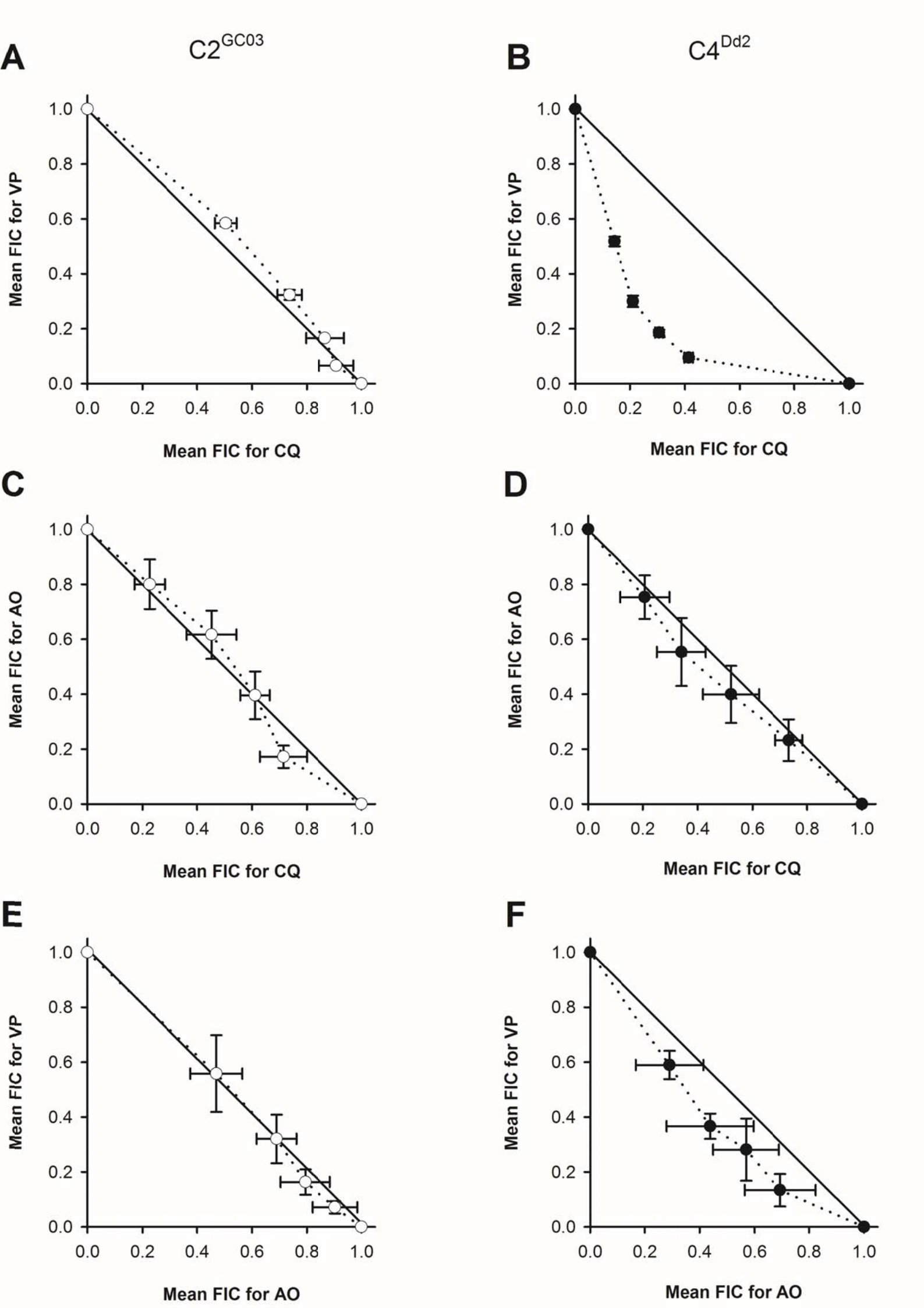
A
C2GC03
B
C4Dd2
C
D
E
F
Mean FIC for VP
Mean FIC for AO
Mean FIC for CQ
0.0
0.2
0.4
0.6
0.8
1.0

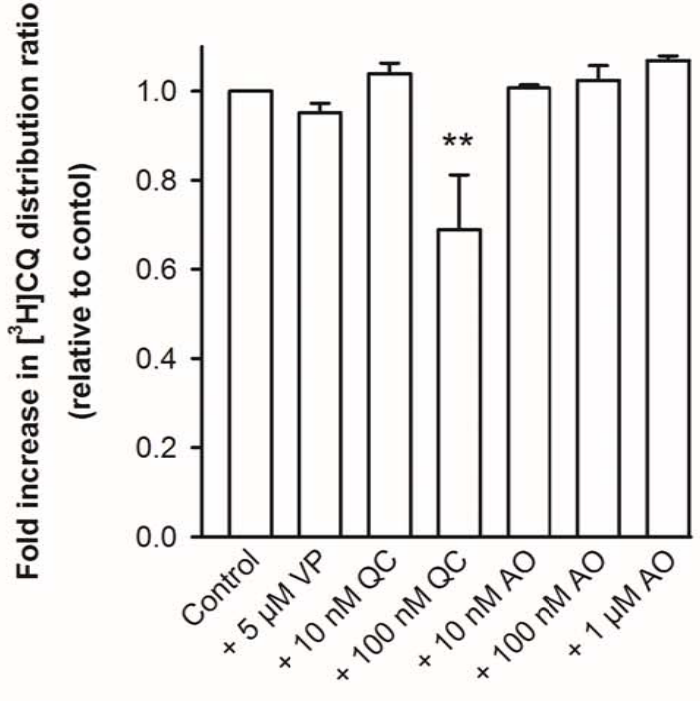
Fold increase in [3H]CQ distribution ratio
(relative to contol)
1.0
0.8
0.6
0.4
0.2
0.0
**
Control
+ 5 μM VP
+ 10 nM QC
+ 100 nM QC
+ 10 nM AO
+ 100 nM AO
+ 1 μM AO

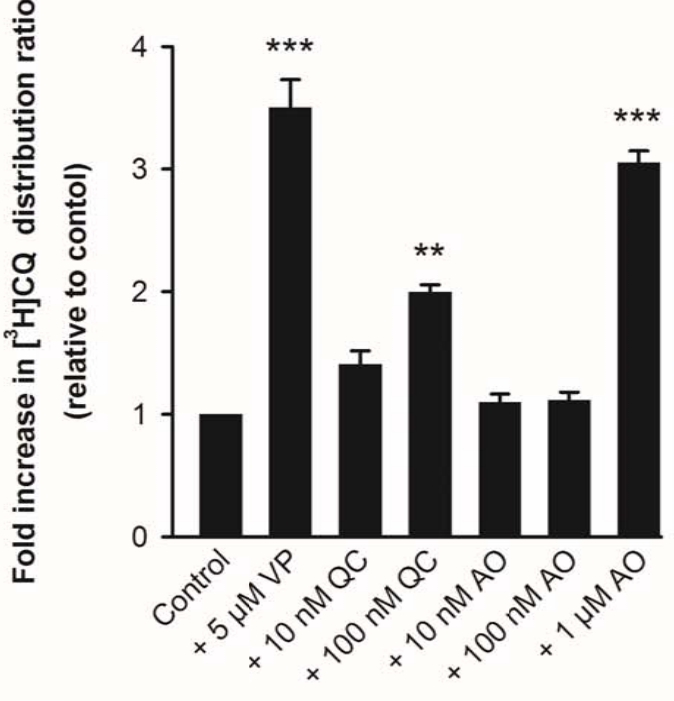
Fold increase in [3H]CQ distribution ratio
(relative to contol)
4
3
2
1
0
***
**
***
Control
+ 5 μM VP
+ 10 nM QC
+ 100 nM QC
+ 10 nM AO
+ 100 nM AO
+ 1 μM AO

B

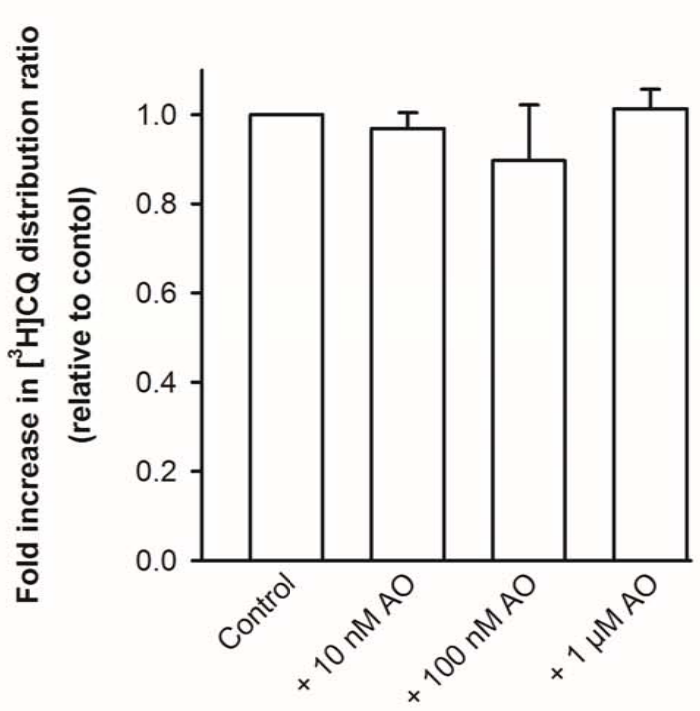
D10
Fold increase in [3H]CQ distribution ratio
(relative to contol)
1.0
0.8
0.6
0.4
0.2
0.0
Control
+ 10 nM AO
+ 100 nM AO
+ 1 μM AO

E

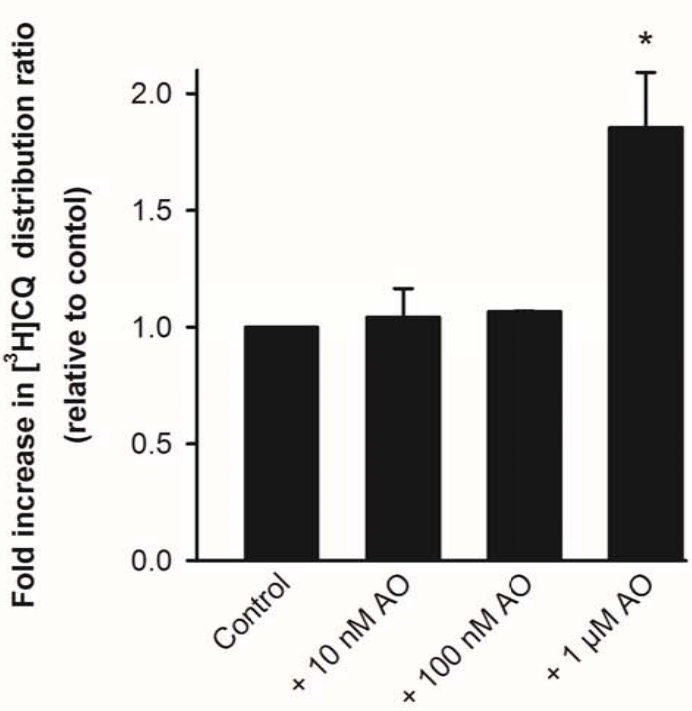
RSA11
Fold increase in [3H]CQ distribution ratio
(relative to contol)
2.0
1.5
1.0
0.5
0.0
*
Control
+ 10 nM AO
+ 100 nM AO
+ 1 μM AO

C

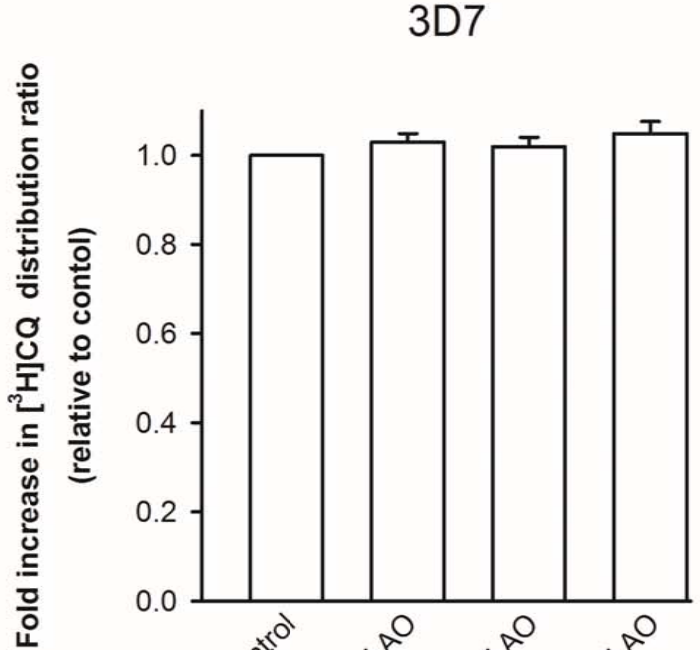
3D7
Fold increase in [3H]CQ distribution ratio
(relative to contol)
1.0
0.8
0.6
0.4
0.2
0.0

F

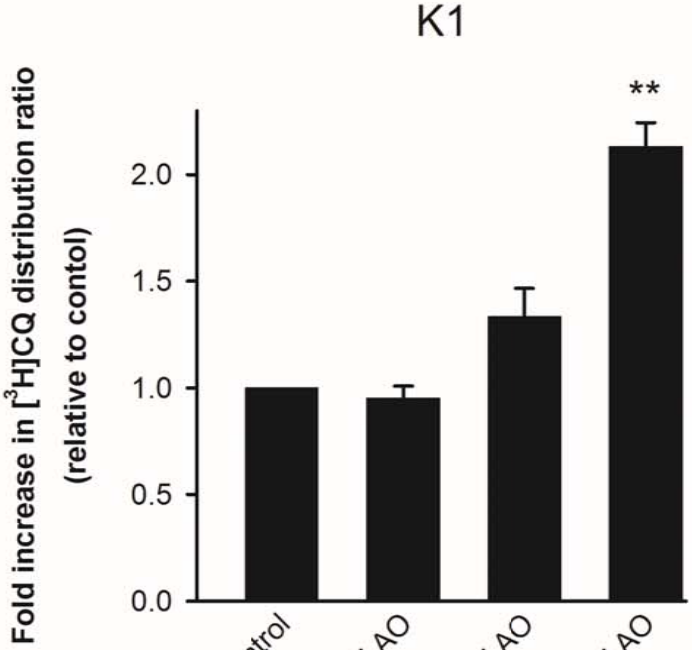
K1
Fold increase in [3H]CQ distribution ratio
(relative to contol)
2.0
1.5
1.0
0.5
0.0
**

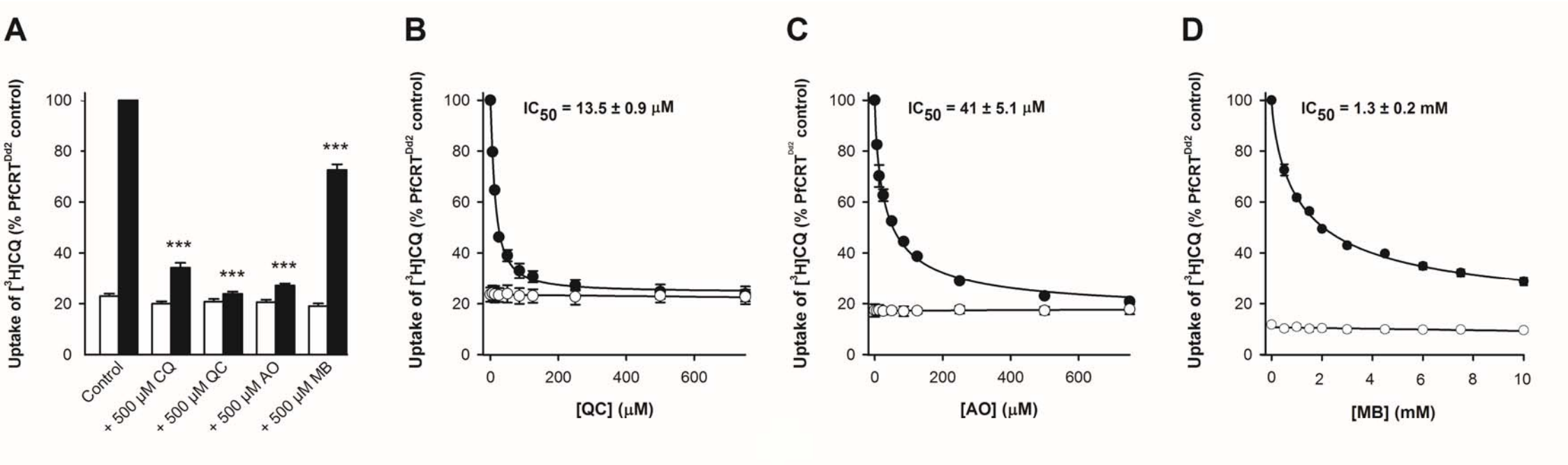
A
Uptake of [3H]CQ (% PfCRTDd2 control)
100
80
60
40
20
0
***
***
***
***
Control
+ 500 µM CQ
+ 500 µM QC
+ 500 µM AO
+ 500 µM MB
B
Uptake of [3H]CQ (% PfCRTDd2 control)
IC50 = 13.5 ± 0.9 µM
0
200
400
600
[QC] (µM)
C
Uptake of [3H]CQ (% PfCRTDd2 control)
IC50 = 41 ± 5.1 µM
0
200
400
600
[AO] (µM)
D
Uptake of [3H]CQ (% PfCRTDd2 control)
IC50 = 1.3 ± 0.2 mM
0
2
4
6
8
10
[MB] (mM)

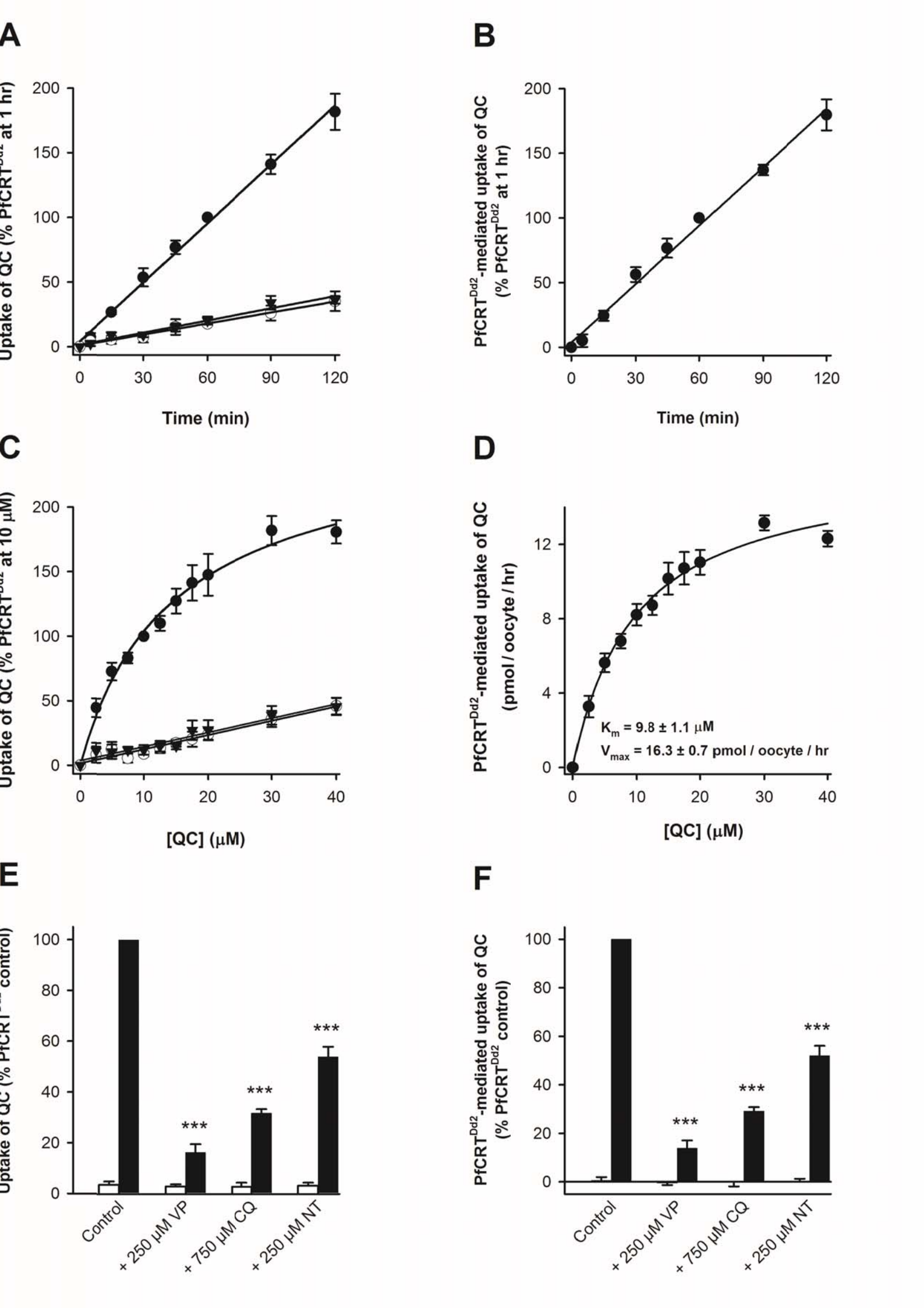
A
Uptake of QC (% PfCRT^{Dd2} at 1 hr)
Time (min)
B
PfCRT^{Dd2}-mediated uptake of QC (% PfCRT^{Dd2} at 1 hr)
Time (min)
C
Uptake of QC (% PfCRT^{Dd2} at 10 μM)
[QC] (μM)
D
PfCRT^{Dd2}-mediated uptake of QC (pmol / oocyte / hr)
K_m = 9.8 ± 1.1 μM
V_{max} = 16.3 ± 0.7 pmol / oocyte / hr
[QC] (μM)
E
Uptake of QC (% PfCRT^{Dd2} control)
***
Control
+ 250 μM VP
+ 750 μM CQ
+ 250 μM NT
F
PfCRT^{Dd2}-mediated uptake of QC (% PfCRT^{Dd2} control)
***
Control
+ 250 μM VP
+ 750 μM CQ
+ 250 μM NT

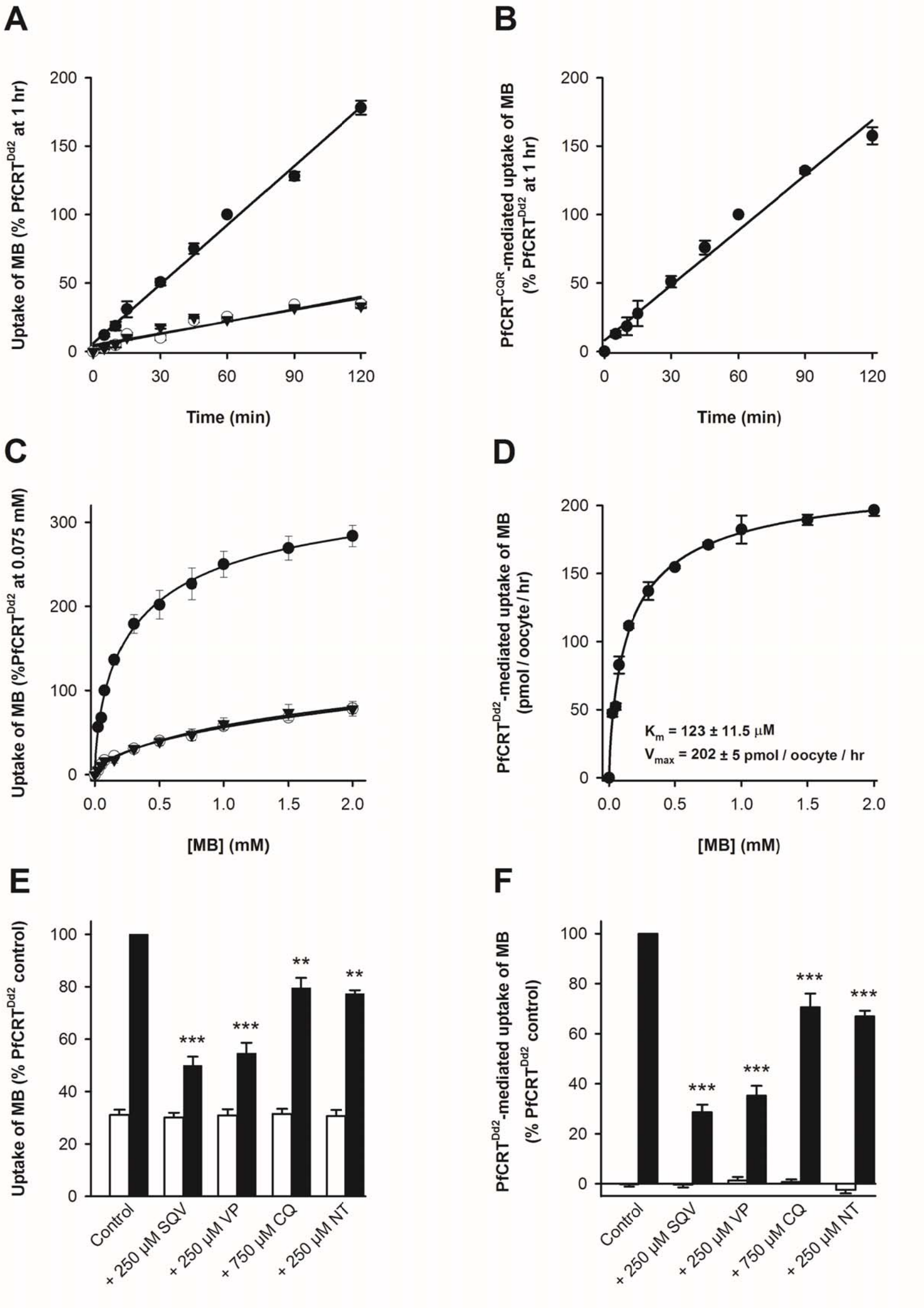
A
Uptake of MB (% PfCRT^Dd2 at 1 hr)
200
150
100
50
0
0
30
60
90
120
Time (min)
B
PfCRT^CQR-mediated uptake of MB (% PfCRT^Dd2 at 1 hr)
200
150
100
50
0
0
30
60
90
120
Time (min)
C
Uptake of MB (%PfCRT^Dd2 at 0.075 mM)
300
200
100
0
0.0
0.5
1.0
1.5
2.0
[MB] (mM)
D
PfCRT^Dd2-mediated uptake of MB (pmol / oocyte / hr)
200
150
100
50
0
K_m = 123 ± 11.5 μM
V_max = 202 ± 5 pmol / oocyte / hr
0.0
0.5
1.0
1.5
2.0
[MB] (mM)
E
Uptake of MB (% PfCRT^Dd2 control)
100
80
60
40
20
0
***
***
**
**
Control
+ 250 μM SQV
+ 250 μM VP
+ 750 μM CQ
+ 250 μM NT
F
PfCRT^Dd2-mediated uptake of MB (% PfCRT^Dd2 control)
100
80
60
40
20
0
***
***
***
***
Control
+ 250 μM SQV
+ 250 μM VP
+ 750 μM CQ
+ 250 μM NT

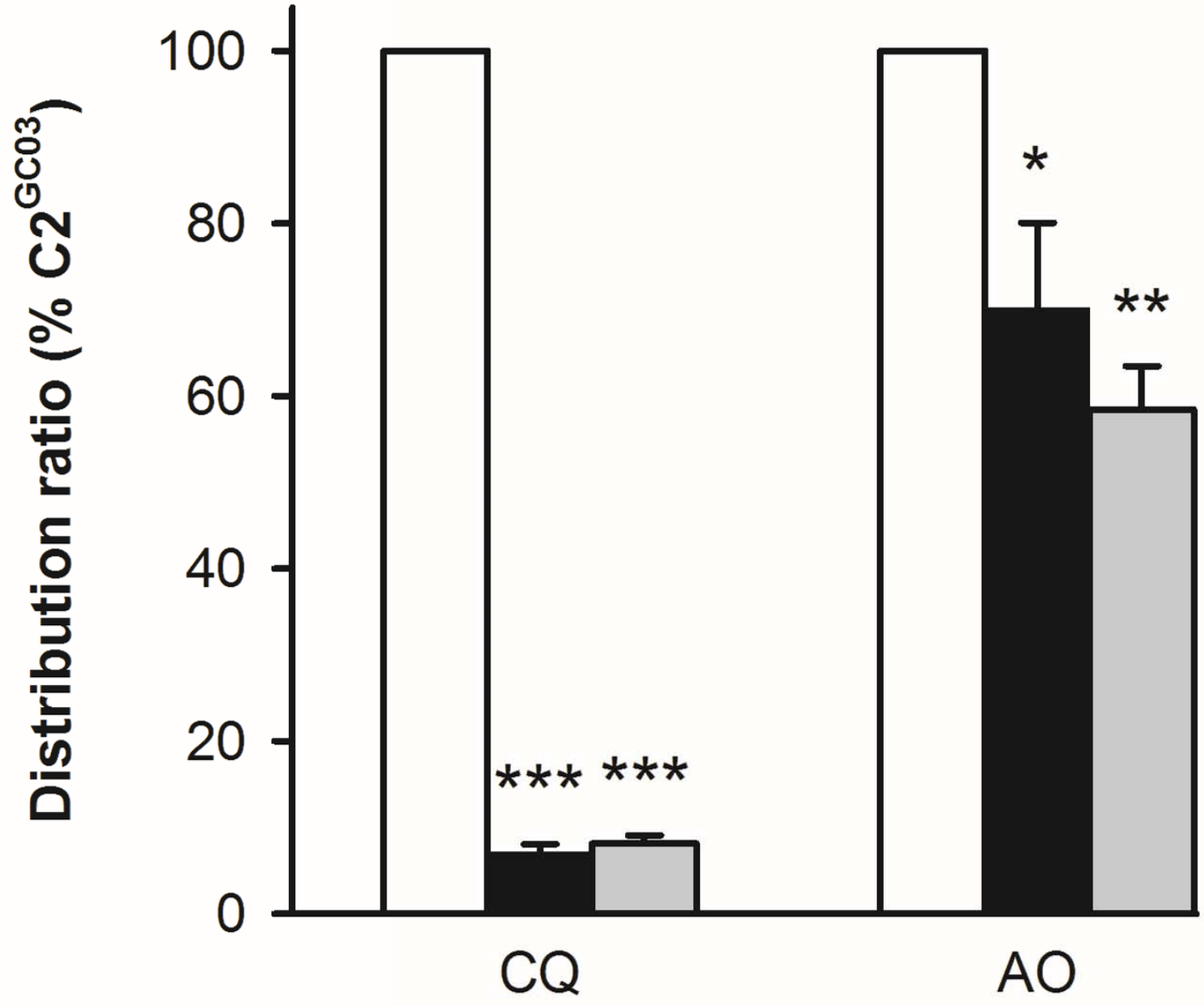
Distribution ratio (% C2GC03)
100
80
60
40
20
0
***
***
*
**
CQ
AO

Table

Table 1. In Vitro Antiplasmodial Activities of Chloroquine (CQ), Quinacrine (QC), Acridine Orange (AO), and Methylene Blue (MB) against CQ-Sensitive and CQ-Resistant *P. falciparum* Parasites

Strain/ line[b]	IC_{50} (nM)[a]							
	Chloroquine		Quinacrine		Acridine orange		Methylene blue	
	Control	+ 1 µM VP	Control	+ 1 µM VP	Control	+ 1 µM VP	Control	+ 1 µM VP
D10	26 ± 2.6	27 ± 2.5	-	-	288 ± 20	283 ± 63	-	-
3D7	21 ± 0.5	20 ± 0.6	9.8 ± 0.2	9.9 ± 0.2	309 ± 34	294 ± 24	2.6 ± 0.04	2.5 ± 0.08
RSA11	354 ± 39[c]	43 ± 5.5[f]	-	-	586 ± 39[e]	563 ± 84	-	-
K1	255 ± 26[c]	63 ± 8.4[f]	-	-	652 ± 42[c]	644 ± 98	-	-
Dd2	142 ± 7.2[c]	26 ± 2.4[f]	16 ± 1.4[d]	7.9 ± 0.6[f]	606 ± 19[d]	549 ± 30	5.3 ± 0.06[c]	2.3 ± 0.08[f]
$C2^{GC03}$	8.3 ± 0.4	8.4 ± 0.2	9.9 ± 0.8	10 ± 0.2	373 ± 28	268 ± 42	2.5 ± 0.03	2.1 ± 0.1
$C4^{Dd2}$	130 ± 9.7[c]	47 ± 8.1[f]	19 ± 0.6[c]	8.9 ± 1.1[f]	592 ± 56[d]	610 ± 27	4.3 ± 0.4[c]	1.9 ± 0.02[f]
$C6^{7G8}$	89 ± 4.1[c]	24 ± 2.9[g]	14 ± 0.8[d]	11 ± 0.2[h]	491 ± 19	501 ± 20	4.7 ± 0.05[c]	2.5 ± 0.03[f]

Abbreviations: IC_{50}, half-maximal inhibitory concentrations; VP, verapamil.

[a]The IC_{50}s are shown as the mean ± SEM from 3 to 11 independent experiments (performed on different days), within which measurements were averaged from 2 or 3 replicates.

[b]Field-derived CQ-sensitive strains: D10 (Papua New Guinea); 3D7 (Africa). Field-derived CQ-resistant strains: RSA11 (South Africa); K1 (Thailand); Dd2 (Indochina/Laos). Isogenic *pfcrt* transfectant lines: $C2^{GCO3}$ (CQ-sensitive); $C4^{Dd2}$ (CQ-resistant); $C6^{7G8}$ (CQ-resistant).

P values determined from Student *t*-test comparisons with the relevant CQ-sensitive strain or line (and within the same drug treatment) were less than [c]0.001, [d]0.01, or [e]0.05.

P values determined from Student *t*-test comparisons with the control treatment from the same CQ-sensitive strain or line (and within the same drug treatment) were less than [f]0.001, [g]0.01, or [h]0.05.

Supplementary Materials for

Verapamil-sensitive transport of quinacrine and methylene blue via mutant PfCRT reduces the malaria parasite's susceptibility to these tricyclic drugs

*Donelly A. van Schalkwyk[a], Megan N. Nash[a], Sarah H. Shafik[a], Robert L. Summers, Adele M. Lehane, Peter J. Smith, and Rowena E. Martin**

[a]D. A. vS., M. N. N., and S. H. S. contributed equally to this work.

*Correspondence: Rowena Martin, Research School of Biology, Australian National University, Canberra, ACT, 2601, Australia (rowena.martin@anu.edu.au).

This PDF file includes:

Supplementary Materials and Methods

Measurements of *P. falciparum* Drug Susceptibility

Parasite proliferation was measured in 96-well plates using either the [^{3}H]hypoxanthine incorporation method or the lactate dehydrogenase (pLDH) assay. The [^{3}H]hypoxanthine incorporation assay was performed over 72 hours using a protocol described elsewhere [1], and the starting hematocrit and parasitemia were both approximately 1%. The Malstat™ reagent (Flow Inc.) was used to measure pLDH activity in accordance with the method of Makler and colleagues [2], and these assays were performed over 48 hours with a starting hematocrit and parasitemia of approximately 1% and 2%, respectively. The level of parasite proliferation in the presence of each drug concentration was expressed as a percentage of the proliferation measured in the absence of drug. The IC_{50} (i.e., the concentration of drug at which the inhibition of parasite growth is half-maximal) was determined in SigmaPlot by a least-squares fit of the equation $y = a/[1+([drug]/IC_{50})c]$ to the data, where y is the percent parasite proliferation, a is the maximum change in the percent parasite proliferation, and c is a fitted constant. The IC_{50}s obtained using the [^{3}H]hypoxanthine incorporation method were indistinguishable from those generated with the pLDH assay.

Antimalarial drug combinations were assessed using fixed-ratio isobolograms [3] as described previously [4]. Fractional inhibitory concentrations (FICs) were calculated for each drug within a combination as follows: FIC (A) = the IC_{50} for drug A in a combination divided by the IC_{50} for drug A alone; FIC (B) = the IC_{50} for drug B in a combination divided by the IC_{50} for drug B alone. The isobolograms were constructed by plotting FIC (A) against FIC (B) for each combination. It is generally accepted that a drug combination is synergistic if the FIC is ≤ 0.5, antagonistic if the FIC is ≥ 4.0 [5], and additive if the FIC is not significantly different from 1.

In all cases, at least three independent experiments were performed (on different days), and within each experiment measurements were averaged from three replicates.

P. falciparum Drug Accumulation Assays

The accumulation of [^{3}H]CQ and [^{3}H]AO was measured in mature trophozoite-infected erythrocytes (~36 hours post-invasion). In the experiments giving rise to the data presented in Figure 2, hematocrit and parasitaemia were approximately 1% and 5%, respectively, and the initial extracellular concentration of [^{3}H]CQ was 2 nM (7 Ci/mmol; Moravek Biochemicals). Prior to the addition of [^{3}H]CQ, the cell suspension was incubated for 15 minutes at 37°C in the presence or absence of the test compound (unlabelled VP, AO, or QC). The 1-hour incubation was terminated by the addition of 100 µL of dibutyl phthalate to the cell suspension and immediate centrifugation (17000 × g, 1 minute) to sediment the cells. The supernatant solution was aspirated and the microcentrifuge tube tip containing the pelleted cells was cut off and placed in a scintillation vial (PerkinElmer). The cells were lysed with 100 µL of Solvable (Packard; 30 minutes at room temperature) and the sample decolourised by the addition of 100 µL of hydrogen peroxide (Sigma; 30 minutes at room temperature). Scintillation fluid (2 mL of Ultima Gold; PerkinElmer) was added to each vial and the samples were shaken overnight. The radioactivity was measured with a Packard Tri-Carb 4640 liquid scintillation analyser. The data presented in panels *A* and *D* of Figure 2 were derived from three independent experiments (performed on different days), within which measurements were averaged from three replicates. Panels *B*, *C*, *E*, and *F* of Figure 2 show the mean of two independent experiments (performed on different days), within which measurements were averaged from three replicates.

The experiments giving rise to the data presented in Figure 6 and Supplementary Figure 3 were performed according to a protocol described in detail elsewhere [6] with minor modifications. Briefly, the hematocrit was 2% and the parasitaemia ranged between 3.2 and

8.4%, and the initial extracellular concentrations of [^{3}H]CQ (20 Ci/mmol) and [^{3}H]AO (25 Ci/mmol) (both from American Radiolabeled Chemicals, ARC) were 20 nM and 50 nM, respectively. The 1-hour incubation at 37°C was terminated by transferring an aliquot of the suspension (200 μL, in duplicate) to a microcentrifuge tube containing 300 μL of dibutyl phthalate (Sigma-Aldrich), which was centrifuged immediately (17,000 × *g*, 2 minutes) to sediment the cells. The supernatant solution was removed by aspiration and residual radioactivity on the sides of the tube was removed by rinsing four times with water, after which the majority of the dibutyl phthalate was aspirated. The cell pellet was dissolved in 1 M NaOH (100 μL, 2 hours at 55°C) and the sample decolourised by the addition of 12.5% w/v bleach (25 μL, 2 hours at room temperature) prior to dilution with water (1 mL). The sample was then transferred to a scintillation vial, mixed with scintillation fluid (1.5 mL of Irga-Safe Plus; PerkinElmer), and the radioactivity measured with a PerkinElmer Tri-Carb 2810 liquid scintillation analyser. The data presented in Figure 6 were derived from four independent experiments (performed on different days), within which measurements were averaged from two replicates.

In all cases, the drug accumulation ratio (i.e., the concentration of [^{3}H]drug within the infected cells relative to the concentration in the extracellular medium) was calculated using a previous estimate of the water volume of a trophozoite-infected erythrocyte (75 fL) [7].

Harvest, Preparation and Microinjection of *X. laevis* Oocytes

Ethical approval of the work performed with the *X. laevis* frogs was obtained from the Australian National University Animal Experimentation Ethics Committee (Animal Ethics Protocol Number A2013/13) in accordance with the Australian Code of Practice for the Care and Use of Animals for Scientific Purposes. Sections of ovary were surgically removed using a procedure adapted from the Laboratory *Xenopus* handbook [8]. Adult female *X. laevis* frogs (purchased from NASCO) were anaesthetised by submersion in a solution of ethyl 3-

aminobenzoate methanesulfonate salt (1.6 g/L of tap water; Sigma-Aldrich) and 1 mM $NaHCO_3$ (Sigma-Aldrich). Anaesthesia was complete after approximately 20 minutes, or when the frog could be turned onto its back without eliciting a response. The frog was then placed onto a container of ice covered with two sheets of moist paper towel. A moist sheet of paper towel was also placed over the frog's head and another over its legs, leaving the abdomen exposed. Ice was piled onto the frog's head and legs to prevent bleeding. After the abdomen was swabbed with a cotton bud sprayed with 80% ethanol, a sterile scalpel was used to make a 1 cm incision directly above the position of an ovary – first through the skin and then though the muscle layer. Sections of the ovary were removed with sterile, surgical-grade tweezers and scissors and placed in a pre-weighed petri dish containing 'calcium-free oocyte ringer' (OR^{2-}) buffer (82.5 mM NaCl, 2.5 mM KCl, 1 mM $MgCl_2$, 1 mM Na_2HPO_4, 5 mM HEPES; pH 7.8). The incision was closed with one stitch of absorbable suture (B. Braun) in the muscle layer, and two stiches of non-absorbable suture (B. Braun) in the skin layer. The wound was swabbed with a cotton bud sprayed with 80% ethanol, after which the frog was returned to an empty tank. The frog then recovered under a sheet of moist paper towel, and was submersed in tap water once fully awake.

The petri dish was re-weighed and the mass of the ovary calculated. The ovary sections were cut into pieces containing around 200 oocytes. If the total mass of the ovary tissue was 17 g or less, the sections were transferred to a 100 mL Erlenmeyer flask, whereas a 250 mL Erlenmeyer flask was used when the total mass was greater than 17 g. The ovary pieces were washed with OR^{2-} buffer (five times, or until the buffer was no longer cloudy) before being incubated for 16 hours at 16°C on an orbital shaker in OR^{2-} buffer supplemented with 0.5 M Na_2HPO_4 (Sigma-Aldrich), bovine serum albumin (250 mg/mL, Sigma-Aldrich), and collagenase D (Roche). The volume of the buffer was 25 mL and 50 mL for the 100 mL and 250 mL flasks, respectively. The amount of collagenase D added to the solution was described by the equation $y = 0.44x + 11.5$, where x was the mass of ovary tissue in g and y was the mass

of collagenase in mg. This ratio of collagenase D to ovary mass typically produced good yields of healthy, single, and de-folliculated oocytes when the ovary mass ranged from 11 to 24 g. The collagenase-treated oocytes were washed ten times with OR^{2-} buffer and five times with 'calcium-containing oocyte ringer' (OR^{2+}) buffer (OR^{2-} buffer supplemented with 1 mM $CaCl_2$ and 50 μg/mL gentamycin). An ovary mass of 14-20 g usually yielded 2000-5000 healthy, de-folliculated oocytes of a suitable size and age (developmental stages V and VI) for microinjection with cRNA (20 ng per oocyte) encoding PfCRT. The injections were performed using a Nanoliter 2000 Injector and Micro4 Controller (World Precision Instruments) with fine-tipped glass capillaries that were shaped on a Flaming/Brown micropipette puller (Sutter Instrument Co.). Oocytes were stored at 16-18°C in OR^{2+} buffer (which was replaced daily) and the solute uptake experiments were performed 3-6 days post-injection.

Measurements of Drug Transport in *Xenopus* Oocytes

The direction of drug transport in the PfCRT oocyte expression system is from the acidic extracellular medium (pH 5.0 to 6.0) into the oocyte cytosol (pH 7.2) [9], which corresponds to the efflux of drug from the acidic digestive vacuole (pH 5 to 5.5) [10-12] into the parasite cytosol (pH 7.3) [13]. A key advantage of this system is that it allows PfCRT to be studied directly and in isolation, without confounding effects such as the binding of drugs to heme or interactions of the compound with other targets or transporters.

Unless specified otherwise, the drug influx assays were performed over 1-2 hours at 27.5°C and in ND96 buffer (96 mM NaCl, 2 mM KCl, 1 mM $MgCl_2$, 1.8 mM $CaCl_2$, 10 mM MES, and 10 mM Tris-base). The uptake of [^{3}H]CQ (0.25 μM; 20 Ci/mmol; ARC) was measured at pH 6.0 and in the presence of 15 μM unlabelled CQ. A subset of experiments attempted to measure the transport of [^{3}H]AO (0.2 μM; 25 Ci/mmol; ARC) into oocytes in the presence of unlabelled AO (1, 2.5, 5, or 10 μM) at pH 4.5, 5.0, 5.5, and 6.0. For each treatment, 10 oocytes were transferred to a 5 mL polystyrene round bottom tube (Falcon) and washed twice with

3.5 mL of ND96 buffer, with the residual buffer removed by pipette. Influx commenced with the addition of 100 µL of ND96 buffer supplemented with [^{3}H]CQ (or [^{3}H]AO), unlabelled CQ (or AO) and, where specified, an unlabelled inhibitor (e.g., QC, AO, MB, or VP). The assay was terminated by removing the reaction buffer with a pipette and washing the oocytes twice with 3.5 mL of ice-cold ND96 buffer. Each oocyte was transferred to a separate scintillation vial and incubated overnight at room temperature in 200 µL of 10% SDS (Sigma-Aldrich). The lysed oocyte was then combined with 1.5 mL of Irga-Safe Plus and the radioactivity measured with a PerkinElmer Tri-Carb 2810 liquid scintillation analyser.

The IC_{50} values presented in Figures 3B-D were determined in SigmaPlot by a least-squares fit of the equation $y = y_{min} + [(y_{max} - y_{min})/(1 + ([\text{inhibitor}]/IC_{50})c]$ to the data, where y is $PfCRT^{Dd2}$-mediated CQ transport, y_{min} and y_{max} are the minimum and maximum values of y, and c is a fitted constant. $PfCRT^{Dd2}$-mediated CQ transport was calculated by subtracting the uptake measured in oocytes expressing $PfCRT^{D10}$ from that in oocytes expressing $PfCRT^{Dd2}$. Note that non-injected oocytes and oocytes expressing $PfCRT^{D10}$ take up [^{3}H]CQ to similar (low) levels via simple diffusion of the neutral species; this represents the 'background' level of CQ accumulation in oocytes (refer to [9] for full data and a detailed discussion).

The influx of unlabelled QC (10 or 40 µM) and MB (75 µM) was detected using the intrinsic fluorescence of these drugs and the uptake assays were performed at pH 6.0 and pH 5.0, respectively. The composition of the pH 5.0 ND96 buffer was 96 mM NaCl, 2 mM KCl, 1 mM $MgCl_2$, 1.8 mM $CaCl_2$, and 20 mM homo-PIPES. A subset of experiments attempted to measure the transport of unlabelled AO (75 or 150 µM) at pH 4.5, 5.0, 5.5, and 6.0. The fluorescence-based experiments were performed as described for the radioisotope uptake assays with the following modifications. At the completion of the incubation, the washed oocytes were transferred to separate wells of a flat 96-well plate (NUNC or PerkinElmer) that had been preloaded with 200 µL of 10% SDS. Each plate included a standard curve that consisted of 10 different concentrations of the fluorescent substrate under study, with each

sample being prepared in a 10% SDS solution containing a lysed oocyte (see Supplementary Figure 2). The plates were incubated overnight at room temperature and mixed on an orbital shaker the following day for approximately 5 minutes. The fluorescence intensity was measured using either a BMG Labtech FLUOstar Optima or a Tecan Infinite M1000 PRO plate-reader. The excitation and emission wavelengths were as follows: QC, 440 and 510 nm; AO, 485 and 520 nm; MB, 668 and 682 nm.

The kinetic parameters for QC and MB transport via $PfCRT^{Dd2}$ (Figures 4D and 5D, respectively) were determined in SigmaPlot by a least-squares fit of the Michaelis-Menten equation ($v = V_{max}[substrate]/(K_m + [substrate])$ to the data.

In all cases, at least three independent experiments were performed (on different days and using oocytes from different frogs), and within each experiment measurements were made from 10-12 oocytes per treatment.

Supplementary Table 1. In Vitro Antiplasmodial Activity of Chloroquine (CQ) against 3D7 and K1 *P. falciparum* Parasites in the Absence or Presence of Acridine Orange (AO) or Verapamil (VP).

Strain[b]	IC_{50} (nM)[a]		
	CQ	CQ + 250 nM AO	CQ + 1 μM VP
3D7	17 ± 4	14 ± 5	15 ± 4
K1	131 ± 11	93 ± 14[c]	46 ± 10[c]

Abbreviations: IC_{50}, half-maximal inhibitory concentration.

[a]The IC_{50}s are shown as the mean ± SEM from 3 independent experiments (performed on different days), within which measurements were averaged from 3 replicates.

[b]3D7 is a field-derived CQ-sensitive strain from Africa and K1 is a field-derived CQ-resistant strain from Thailand.

[c]A student *t*-test comparison with the CQ IC_{50} determined for the K1 strain in the absence of AO or VP yielded a *P* value less than 0.05.

Supplementary Table 2. Percentages of Chloroquine, Quinacrine, and Acridine Orange in their Neutral, Monoprotonated (H^+), or Diprotonated (H_2^{2+}) Forms in Solutions of Different pH.

pH	CQ			QC			AO[a]	
	% CQ	% CQH^+	% CQH_2^{2+}	% QC	% QCH^+	% QCH_2^{2+}	% AO	% AOH^+
5.0	0.0000005	0.0799997	99.9199998	0.0000005	0.1261314	99.8738681	0.0015849	99.9984151
5.5	0.0000050	0.2525445	99.7474505	0.0000050	0.3977775	99.6022175	0.0050116	99.9949884
6.0	0.0000497	0.7942781	99.2056722	0.0000495	1.2471555	98.7527951	0.0158464	99.9841536
6.4	0.0003100	1.9714568	98.0282332	0.0003065	3.0747290	96.9249645	0.0397949	99.9602051
6.9	0.0029731	5.9792417	94.0177852	0.0028739	9.1167741	90.8803520	0.1257343	99.8742657
7.4	0.0263210	16.7393496	83.2343294	0.0240013	24.0772048	75.8987939	0.3965286	99.6034714
8.4	1.0392882	66.0955322	32.8651795	0.7522247	75.4603423	23.7874330	3.8286504	96.1713496

The percentages were calculated using the Henderson-Hasselbach equation ($pH = pK_a + \log([A^-]/[HA])$) using the pK_a values shown in Supplementary Figure 1.

Abbreviations: CQ, chloroquine; CQH^+, monoprotonated chloroquine; CQH_2^{2+}, diprotonated chloroquine; QC, quinacrine; QCH^+, monoprotonated quinacrine; QCH_2^{2+}, diprotonated quinacrine; AO, acridine orange; AOH^+, monoprotonated acridine orange.

[a]Note that the concentration of the neutral form of AO at pH 5.0 is 32-fold greater than that of neutral QC at pH 6.0.

Supplementary Figure 1. The structures of the compounds used in this study. Abbreviation: pK_a, the negative logarithm to the base 10 of the acid dissociation constant (K_a).

Chloroquine

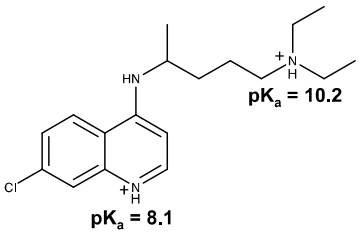

Quinacrine

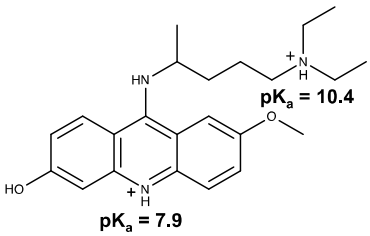

Acridine Orange

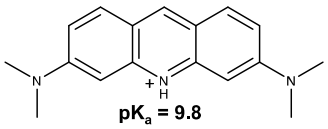

Methylene Blue

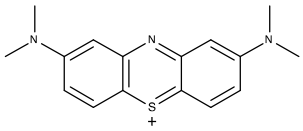

Leuco-Methylene Blue

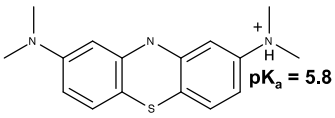

Saquinavir

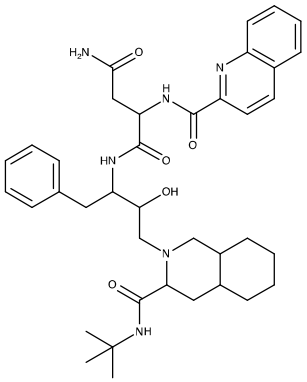

Verapamil

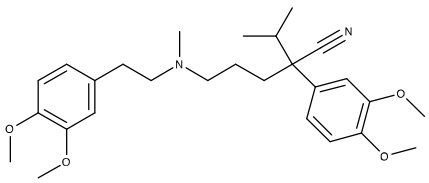

Neurotensin

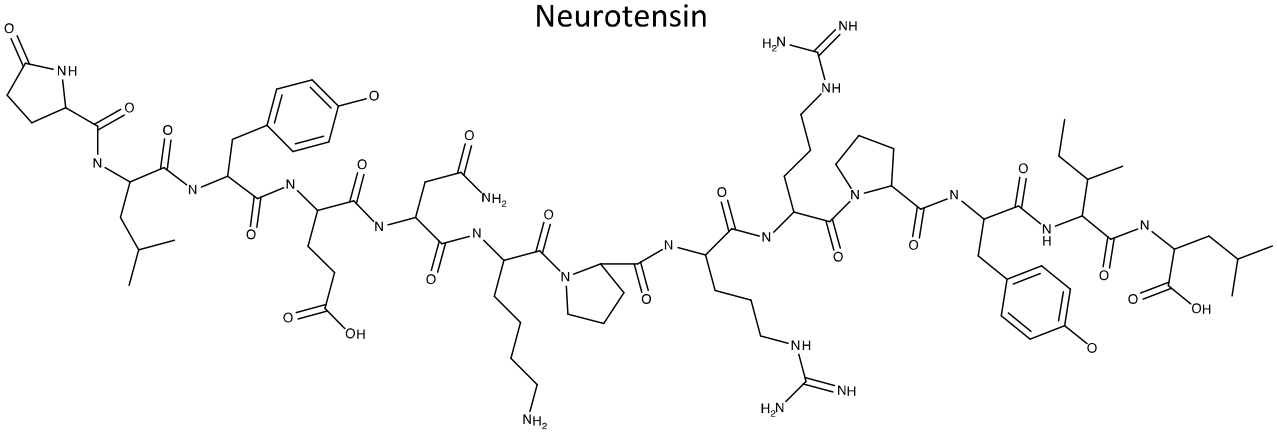

Supplementary Figure 2. The fluorescence intensities of quinacrine (QC), acridine orange (AO), and methylene blue (MB) are linear with concentration in a 10% SDS solution containing a lysed oocyte. The drug influx assays entail dissolving each oocyte in 200 µL of a 10% SDS solution to release the accumulated drug. Given that the resulting oocyte debris could reduce the level of excitation energy that reaches the compound and/or absorb the emitted fluorescence, it was necessary to prepare each concentration standard in 200 µL of a 10% SDS solution that contained a lysed oocyte. *A*, The fluorescence intensity of QC, which was measured at an excitation wavelength of 440 nm and an emission wavelength of 510 nm, was linear with concentration between 0.001 and 1 µM. *B*, The fluorescence intensity of AO, which was measured at an excitation wavelength of 485 nm and an emission wavelength of 520 nm, was linear with concentration between 0.0625 and 2 µM. *C*, The fluorescence intensity of MB, which was measured at an excitation wavelength of 668 nm and an emission wavelength of 682 nm, was linear with concentration between 0.2 and 100 nM. The data represent the mean ± SEM from 3 to 11 independent experiments, performed on different days and using oocytes from different frogs. The error bars for each of the data points fell within the symbols.

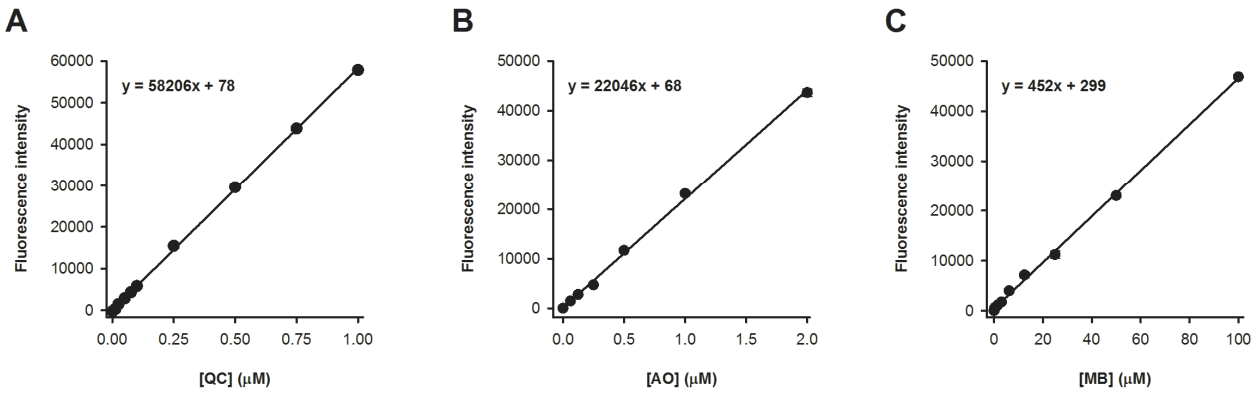

Supplementary Figure 3. The effect of chlorpheniramine (CP) on the accumulation of radiolabelled chloroquine ([^{3}H]CQ) or radiolabelled acridine orange ([^{3}H]AO) by erythrocytes infected with mature trophozoite-stage parasites. The white, black, and gray bars show data for the C2^{GCO3}, C4^{Dd2}, and C6^{7G8} parasite lines, respectively, under control conditions or in the presence of 2.5 μM CP. The accumulation of [^{3}H]drug was expressed as a 'distribution ratio' (i.e., the concentration of [^{3}H]drug within the infected cells relative to the concentration in the extracellular medium) and is shown relative to the ratio measured in the C2^{GCO3} parasites in the absence of CP. The data represent the mean + range/2 of 2 independent experiments (performed on different days), within which measurements were averaged from 2 replicates.

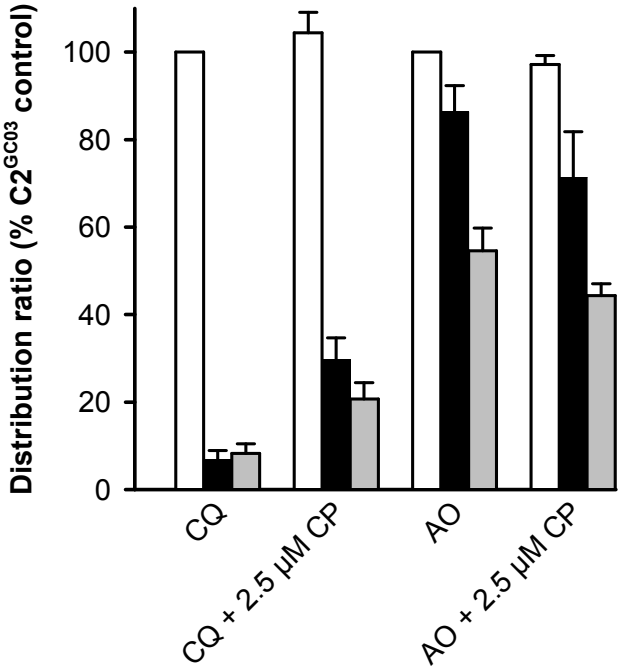

References

1. Desjardins, R.E., C.J. Canfield, J.D. Haynes, J.D. Chulay. Quantitative assessment of antimalarial activity in vitro by a semiautomated microdilution technique. Antimicrob Agents Chemother **1979**; 16:710-8.
2. Makler, M.T., J.M. Ries, J.A. Williams, et al. Parasite lactate dehydrogenase as an assay for *Plasmodium falciparum* drug sensitivity. Am J Trop Med Hyg **1993**; 48:739-41.
3. Fivelman, Q.L., I.S. Adagu, D.C. Warhurst. Modified fixed-ratio isobologram method for studying *in vitro* interactions between atovaquone and proguanil or dihydroartemisinin against drug-resistant strains of *Plasmodium falciparum*. Antimicrob Agents Chemother **2004**; 48:4097-102.
4. van Schalkwyk, D.A., W. Priebe, K.J. Saliba. The inhibitory effect of 2-halo derivatives of D-glucose on glycolysis and on the proliferation of the human malaria parasite *Plasmodium falciparum*. J Pharmacol Exp Ther **2008**; 327:511-7.
5. Odds, F.C. Synergy, antagonism, and what the chequerboard puts between them. J Antimicrob Chemother **2003**; 52:1.
6. Lehane, A.M., D.A. van Schalkwyk, S.G. Valderramos, D.A. Fidock, K. Kirk. Differential drug efflux or accumulation does not explain variation in the chloroquine response of *Plasmodium falciparum* strains expressing the same isoform of mutant PfCRT. Antimicrob Agents Chemother **2011**; 55:2310-8.
7. Saliba, K.J., H.A. Horner, K. Kirk. Transport and metabolism of the essential vitamin pantothenic acid in human erythrocytes infected with the malaria parasite *Plasmodium falciparum*. J Biol Chem **1998**; 273:10190-5.
8. Green, S.L. *The laboratory* Xenopus *sp.* M.A. Suckow ed. 1st ed. Boca Raton: CRC Press, **2010**:136-38.

9. Martin, R.E., R.V. Marchetti, A.I. Cowan, S.M. Howitt, S. Bröer, K. Kirk. Chloroquine transport via the malaria parasite's chloroquine resistance transporter. Science **2009**; 325:1680-2.

10. Hayward, R., K.J. Saliba, K. Kirk. The pH of the digestive vacuole of *Plasmodium falciparum* is not associated with chloroquine resistance. J Cell Sci **2006**; 119:1016-25.

11. Klonis, N., O. Tan, K. Jackson, D. Goldberg, M. Klemba, L. Tilley. Evaluation of pH during cytostomal endocytosis and vacuolar catabolism of haemoglobin in *Plasmodium falciparum*. Biochem J **2007**; 407:343-54.

12. Kuhn, Y., P. Rohrbach, M. Lanzer. Quantitative pH measurements in *Plasmodium falciparum*-infected erythrocytes using pHluorin. Cell Microbiol **2007**; 9:1004-13.

13. Saliba, K.J., K. Kirk. pH regulation in the intracellular malaria parasite, *Plasmodium falciparum*. H^+ extrusion via a V-type H^+-ATPase. J Biol Chem **1999**; 274:33213-9.